3
Optoelectronic Molecular Switches Based on Dihydroazulene-Vinylheptafulvene (DHA-VHF)

Thomas Mrozek, Joerg Daub, and Ayyppanpillai Ajayaghosh

3.1
Introduction

Molecular switches are the active components of molecular electronic devices capable of inducing chemical and physical changes in response to external stimuli such as electrical current, light, and biological impulses.[1] Switching needs selective and fast activation processes, making photons, electrons, phonons, or protons the best means for the supply of energy. An optoelectronic molecular switch is a molecular system possessing electronic properties that can be triggered or controlled with the aid of stimuli such as light or application of electrochemical potential. The most amazing natural process assisted by a photonic switch is the phenomenon of vision in living systems. It is now reasonably well known that rhodopsin undergoes changes in geometry upon optical excitation, altering from the *cis* to the *trans* conformation on a subpicosecond time scale, and that this is responsible for the various switching processes in vision. Over recent years there have been several attempts to design molecular switches with the goal of developing molecular electronic devices, expected to be a key technology of the future.[2] Photoresponsive molecular switches in particular are of great interest, since use of light as an external stimulus allows for rapid and clean interconversions of distinctly different states.[3] Several classes of photoresponsive molecular switches are known, operating through such various processes as reversible bond formation and breaking, *cis–trans* isomerization, photoinduced electron transfer (PET), and proton transfer. PET is one of the most interesting rapid switching mechanisms, allowing for regulation of properties such as luminescence behavior. Fluorescence emission is perhaps the most widely exploited property in the design of PET molecular switches, since it is extremely sensitive to various perturbations: such as solvent polarity, donor-acceptor interactions, and the presence of metal ions. Several such systems have also been used in the design of AND logic gates (Compound **1**) and molecular sensors.[4]

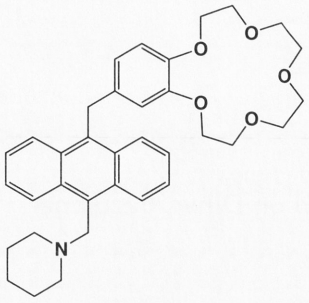

1

Photoredox switches (**P**: photoactive subunit; **R**: redox active subunit) are another important class of molecular switches.[5] Reversible redox interconversion between two different states can result in the switching on and off of luminescence in a two-component system **P-R**. In such a system, switching is achieved when the oxidized or reduced form of **R** induces an electron transfer or energy transfer process to or from the photoexcited subunit **P***; a schematic representation is given in Figure 1. A luminescent redox switch reported by Lehn and co-workers is based on a quinone/hydroquinone moiety attached to a luminescent $(Ru^{II}(bpy)_3)^{2+}$ fragment (Structure **2**).[6] The electron transfer process from the bipyridyl fragment in its excited state to the adjacent quinone moiety quenches luminescence, while reversion to the reduced hydroquinone form results in the restoration of emission (Figure 2/top).

Another example of a photoredox molecular switch is based on a ferrocene-ruthenium trisbipyridyl conjugate, in which the luminescent form **4** switches to the non-luminescent form **5** upon electrochemical oxidation (Figure 2/bottom)[7]. Biological systems exploit the interplay of redox and molecular recognition to regulate a wide variety of processes and transformations. In an attempt to mimic such redox systems, Deans et al. have reported a three-component, two-pole molecular switch, in which noncovalent molecular recognition can be controlled electrochemically.[8] Willner et al. have reported on their research activities in developing novel means to achieve reversible photostimulation of the activities of biomaterials (see Chapter 6).[9] Recently, we have shown that it is possible to switch the luminescence in benzodifuran quinone **6** electrochemically.[10] The reduction in THF of the quinone moiety

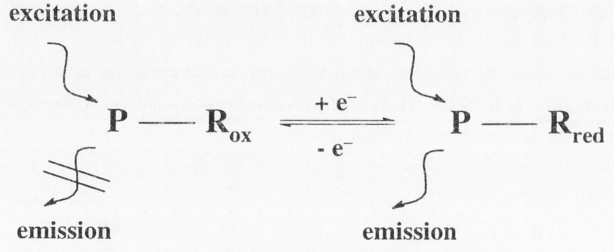

Fig. 1: Schematic representation of photoredox switching; Luminescence quenched in the oxidized state of R (R_{ox}).

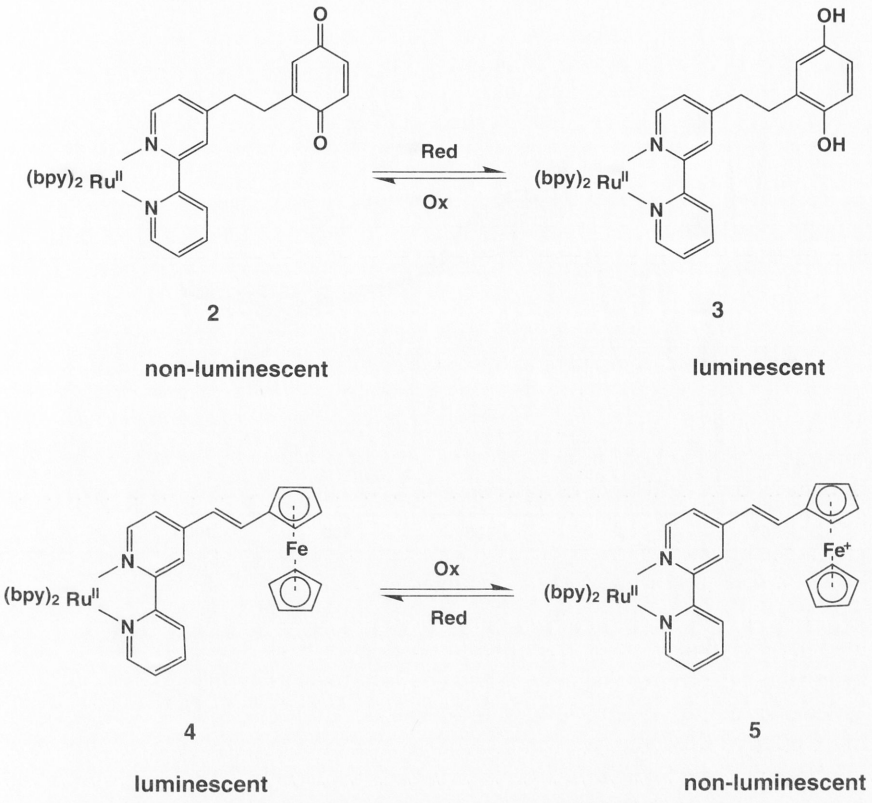

Fig. 2: Redox luminescence switching in trisbipyridyl metal complexes.

to the hydroquinone dianion occurs in a reversible, two-step process at $E_{1/2} = -1223$ mV and –1913 mV. The spectra obtained for the radical anion forms by UV/Vis/NIR spectroelectrochemical measurements agree with the quinone structure, illustrating that the two reversible redox processes are largely localized at the benzodifuran unit (Figure 3/top). The fluorescence spectrum of **6**, which is weak at the beginning of the electrochemical reduction, becomes stronger during the reduction to $\mathbf{6}^{2-}$, as shown in Figure 3/bottom.

Functionalized difluoroboradiaza-s-indacenes have recently been shown to undergo proton-dependent and metal ion-dependent fluorescence switching.[11] For example, compound **7** initially displays a very low fluorescence quantum yield, but, as shown in Figure 4, this is enhanced significantly upon addition of aqueous HCl.[11b] Cyclic voltammetry on **7** indicated that the oxidation of the dimethylamino group, appearing between the oxidation and the reduction of the indacene framework, disappeared upon protonation.[11a] The increase in oxidation potential of the protonated **7** makes the nonradiative deactivation process less efficient, thereby enhancing the efficiency of the fluorescence quantum yield.

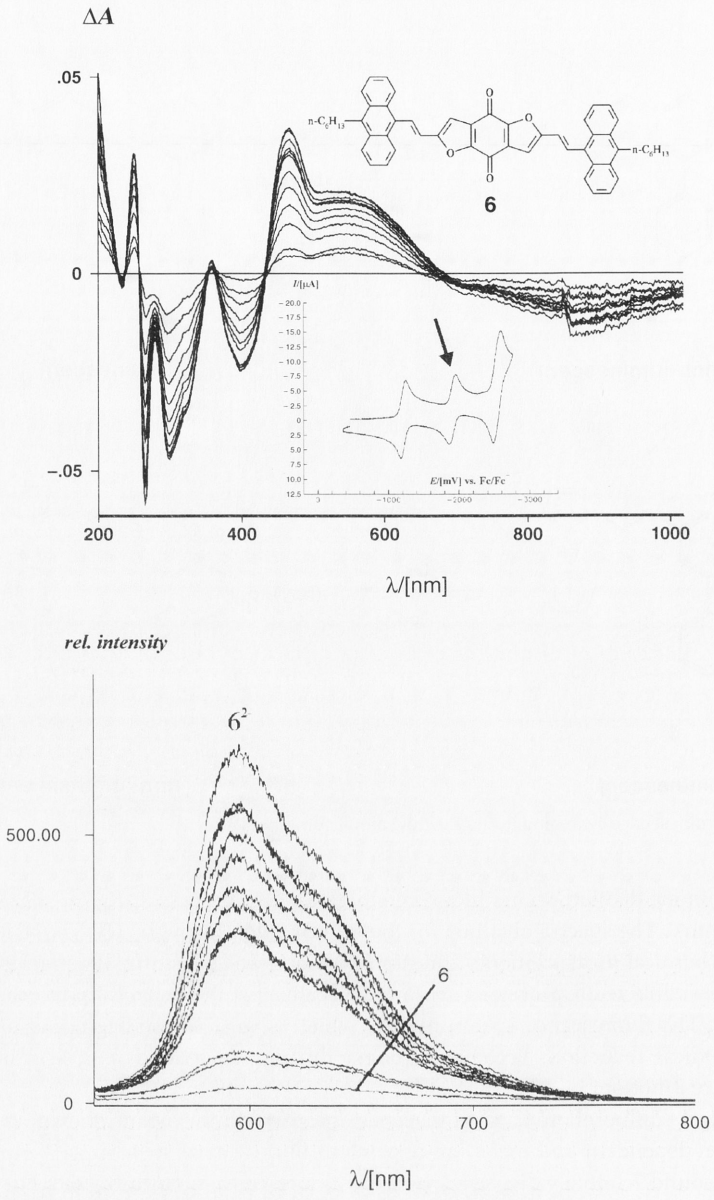

Fig. 3: Top: Difference spectra (referenced to the spectrum of the radical anion $\mathbf{6}^{\bullet-}$) showing the formation of the dianion $\mathbf{6}^{2-}$ from $\mathbf{6}^{\bullet-}$. The cyclic voltammogram is shown in the inset. The applied potential is indicated by the arrow. Bottom: "ON/OFF"-switching of luminescence during reduction of **6**.

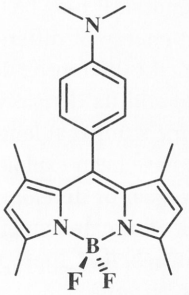

7

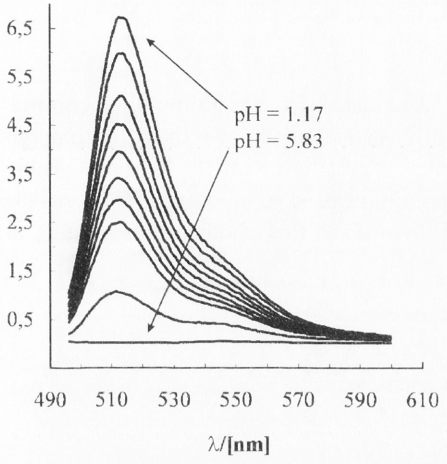

Fig. 4: Effect of pH on the fluorescence switching of compound **7** in a methanol–water mixture (volume fraction [$\phi = 0.5$]). The pH values (in order of decreasing fluorescence intensity) are: 1.17, 2.10, 2.51, 2.65, 3.07, 3.24, 3.37, 3.53, 3.81, and 5.83.

3.2 Photochromic Molecular Switches

Information storage at the molecular level, using switchable molecular devices, is expected to revolutionize information processing and communication systems. Photochromic groups are known to have the potential to reversibly alter the molecular structure, electronic properties, and/or physical characteristics of a substrate attached to them.[3] Therefore, the photochromic behavior of organic molecules can be used to trigger the switching of a required property, which in turn can be exploited in the designing of materials useful for molecular electronic and photonic devices. Because of this, an ever increasing effort is being directed towards designing and studying dynamic molecular systems for utilization as switching devices that can undergo reversible changes between different states. Judicious manipulation of the molecular structures of such systems permits tuning and optimization of the switching behavior for specific applications.

Photochromism is the phenomenon whereby a molecule can exist reversibly in two or more different forms with distinctly different physical or chemical properties, and can be induced to change between them by photochemical means. It may be

due to simple isomerization of a substituted ethylenic double bond, or it may be the result of ring-closure and ring-opening in the presence of light energy of different wavelengths. Several examples of such systems are known in the literature. For example, the well known *cis–trans* isomerization of azobenzene and its derivatives has been extensively studied,[12] while other photochromic systems studied at length include fulgides[13] and diarylethenes[14]. Many of these systems have been exploited for the designing of molecular level switching devices, with the goal of developing viable information storage systems. Before going into the details of dihydroazulene-vinylheptafulvene photochromism and its use in molecular switches, it is appropriate to take a brief look at some of the other known photochromic systems.

3.2.1 Molecular Switches Based on Fulgides

Fulgides and fulgimides are promising candidates for designing photochromic switches (see Chapter 10 for an extensive discussion). It is known that they undergo reversible ring-closure and ring-opening upon irradiation with UV light and visible light respectively, giving rise to the corresponding ***closed*** (***C***) and ***open*** (***O***) ***forms*** (**8**/**9**) (Figure 5).[13] Walz et al. have successfully utilized this photochromic system to

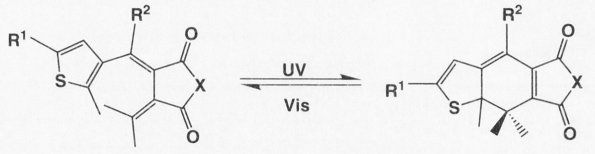

O-isomer ***C***-Isomer

8 **9**

Fig. 5: Photochromism in fulgide (X=O) and fulgimide ($X=NR^3$)-type systems.

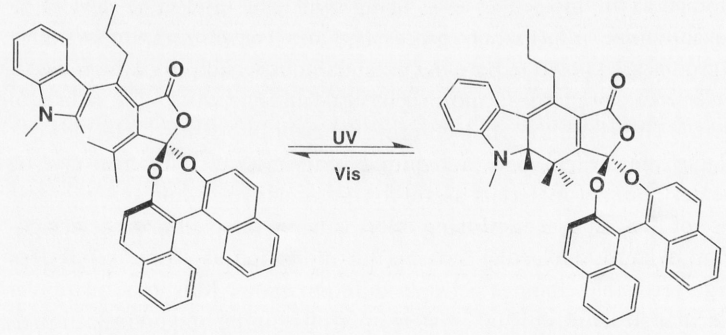

non fluorescent **fluorescent**

10 **11**

Fig. 6: "ON/OFF"-switching of fluorescence in a fulgide-type system.

design molecular switches consisting of a donor-fulgide-acceptor triad[15]. The switching "on" and "off" of the fluorescence of an attached fluorophore depends upon the energy transfer process between a donor and an acceptor, and this in turn depends upon the geometric configuration of the photochromic fulgide, as shown in Figure 5. Inada et al. have reported perfect on-off switching of fluorescence emission in a fulgide photochromic system with an attached binaphthol substituent.[16] While the colorless form of the propyl-substituted binaphthol-condensed indolylfulgide **10** did not display fluorescence, its colored form **11**, obtained on irradiation with UV light, exhibited fluorescence in toluene at room temperature (Figure 6).

3.2.2
Photochromic Switches Based on Dihydroindolizine

Recently, Weber et al. have reported a dual mode molecular switching device with nondestructive readout capability, based on a photochromic dihydroindolizine (**DHI**).[17] The write-lock-read-erase mechanism, as shown in Figure 7, is based on irradiation of **12** to form the colored betaine **13** and its subsequent protonation to **14**. This in turn can undergo deprotonation back to **13** and, finally, thermal reversion to **12**. However, the absorption ranges of the ring-closed **12** and the ring-opened betaine **14** are not optimal, and its use as a data storage system is limited accordingly.

3.2.3
Multimode Molecular Switch Based on Flavylium Ion

The photochromic system constituted by the 4′-hydroxyflavylium ion **15a**, reported by the groups of Pina, Maestri, and Balzani,[18a,b] is an interesting system, being a multistable, multifunctional molecular switch reminiscent in its photoactive *trans*-2,4′-dihydroxychalcone form (**15d**) of **P**hotoactive **Y**ellow **P**rotein (**PYP**), a sensory protein in nature (see also Chapter 10).[18c,d] System **15** (Figure 8) has been found suitable as an optical memory device with multiple storage capability at different memory levels and nondestructive readout capacity through a write-lock-read-unlock-erase cycle. All the observed processes are fully reversible, and are accompanied by large changes in absorption and emission properties.

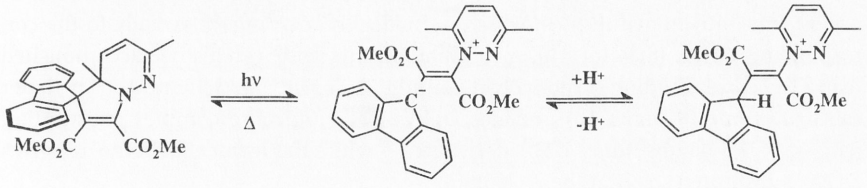

12 13 14

Fig. 7: Light-driven switch represented by dihydroindolizine **12**, betaine **13**, and protonated betaine **14** (Δ = thermal activation).

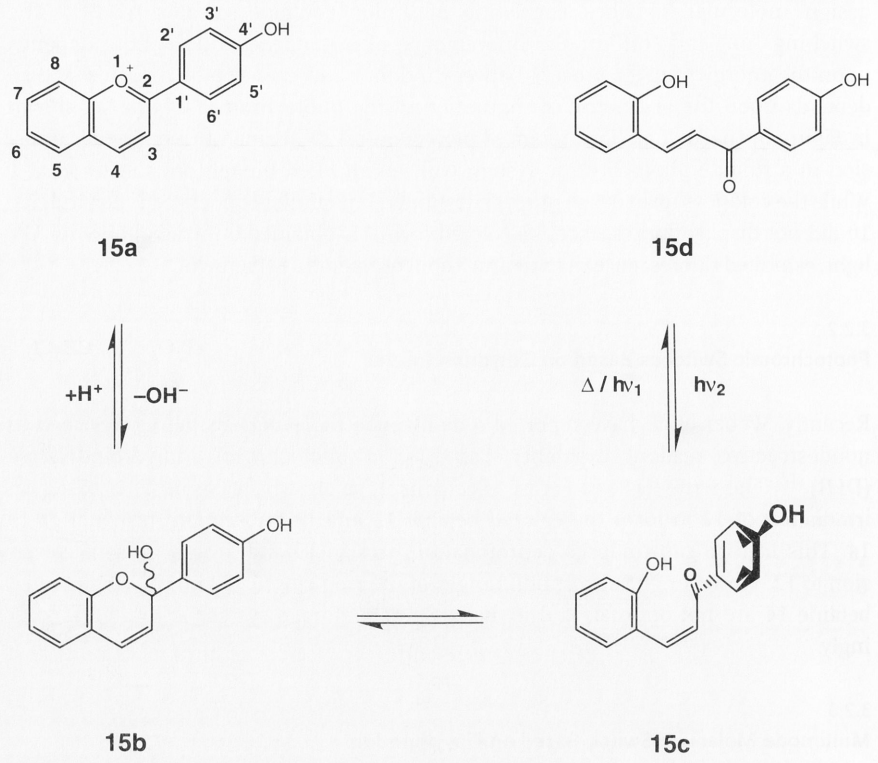

Fig. 8: Structural transformations of the 4′-hydroxyflavylium ion **15a**. Only the important forms are shown.

3.2.4 Dihydroazulene-Vinylheptafulvene Photochromism (DHA-VHF Photochromism)

Dihydroazulenes are alternant π-tetraenic systems, that can be obtained directly by the [8+2] cycloaddition of 8-methoxyheptafulvene with dicyanoethylenes, followed by elimination of methanol (Scheme 1a). An alternative means of preparation is by C–C bond formation between a cycloheptatrienylium cation and an appropriate dicyanoethylene derivative, followed by dehydrogenation to afford the nonalternant π-pentaenic vinylheptafulvenes, which immediately rearrange thermally to the corresponding **DHA**s (Scheme 1b). A variation on this route can also be accomplished using the corresponding carbonyl compounds, as depicted in Scheme 1b. The latter synthetic route (Scheme 1b) provides **DHA**s featuring more complex substitution patterns – 2,3-disubstituted **DHA** derivatives – while the former (Scheme 1a) gives **DHA**s substituted solely at the 2-position.

The **DHA**s undergo an interesting photoinduced rearrangement to the corresponding **VHF**s, and this is accompanied by a change of color from, in the case of the phenyl derivative **18a** (Scheme 2), yellow to dark red.[3a,19] In this case, it was

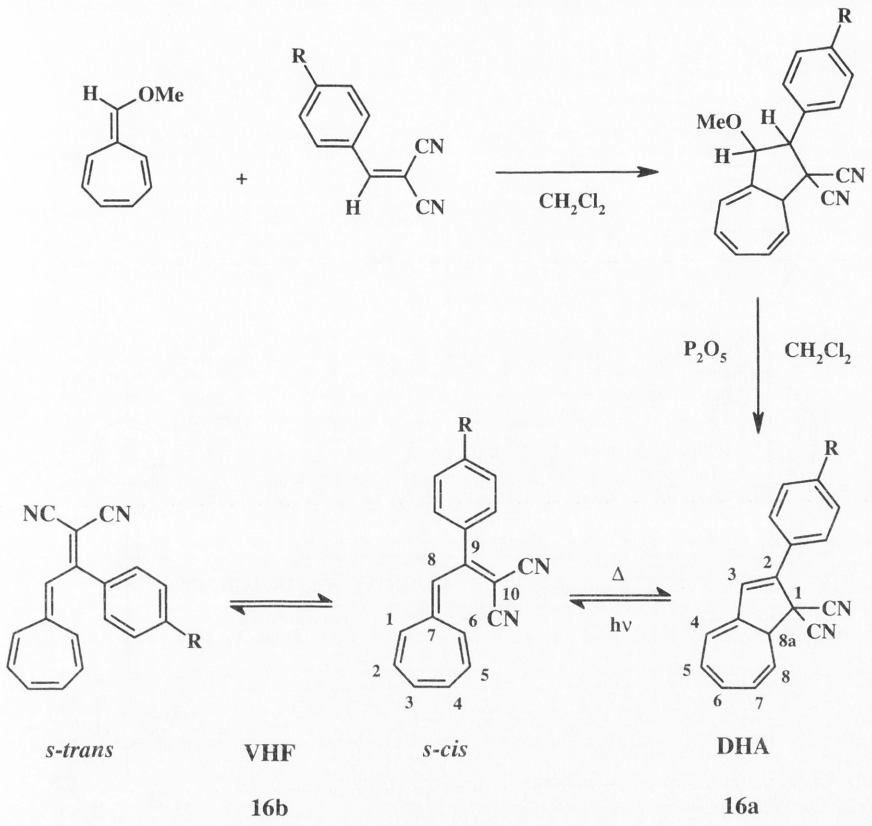

Scheme 1a: 'Direct' pathway for the synthesis of dihydroazulenes.

observed that upon irradiation (in acetonitrile) the intensity of the absorption band at 350 nm decreased while a new, long wavelength absorption at 468 nm was formed through four isosbestic points (Figure 9). The **VHF 18b** underwent quantitative thermal reversion to the **DHA 18a** within 70 h at 25 °C. The quantitative conversions of the photochemical forward reaction and the thermal back reaction could be followed by ^{1}H NMR spectral studies. The photoreaction occurs from the excited singlet state; the quantum yield of the reaction was 0.55. The rate constant for the thermal back reaction at 25 °C was found to be 7×10^{-5} s^{-1}.

The photochromic properties of **DHA** systems depend strongly upon the substituents on the five-membered ring, the reaction media, and the temperature. For example,[20] to obtain a steady state equilibrium mixture of **22a** and **22b** (Scheme 3), the 2,4-dinitrophenyl derivative of the **DHA 22a** had to be irradiated (in acetonitrile, 366 nm irradiation wavelength) at low temperature (200 K). In contrast to this, arene derivatives **21a** and **23a**, on irradiation at 250 K, were quantitatively converted to the corresponding **VHFs 21b** and **23b**, respectively. In the case of the **DHA 24a**, a stationary equilibrium between **24a** and **24b** could be observed at room temperature. Thus, in general, it was observed that the presence of electron-withdrawing substitu-

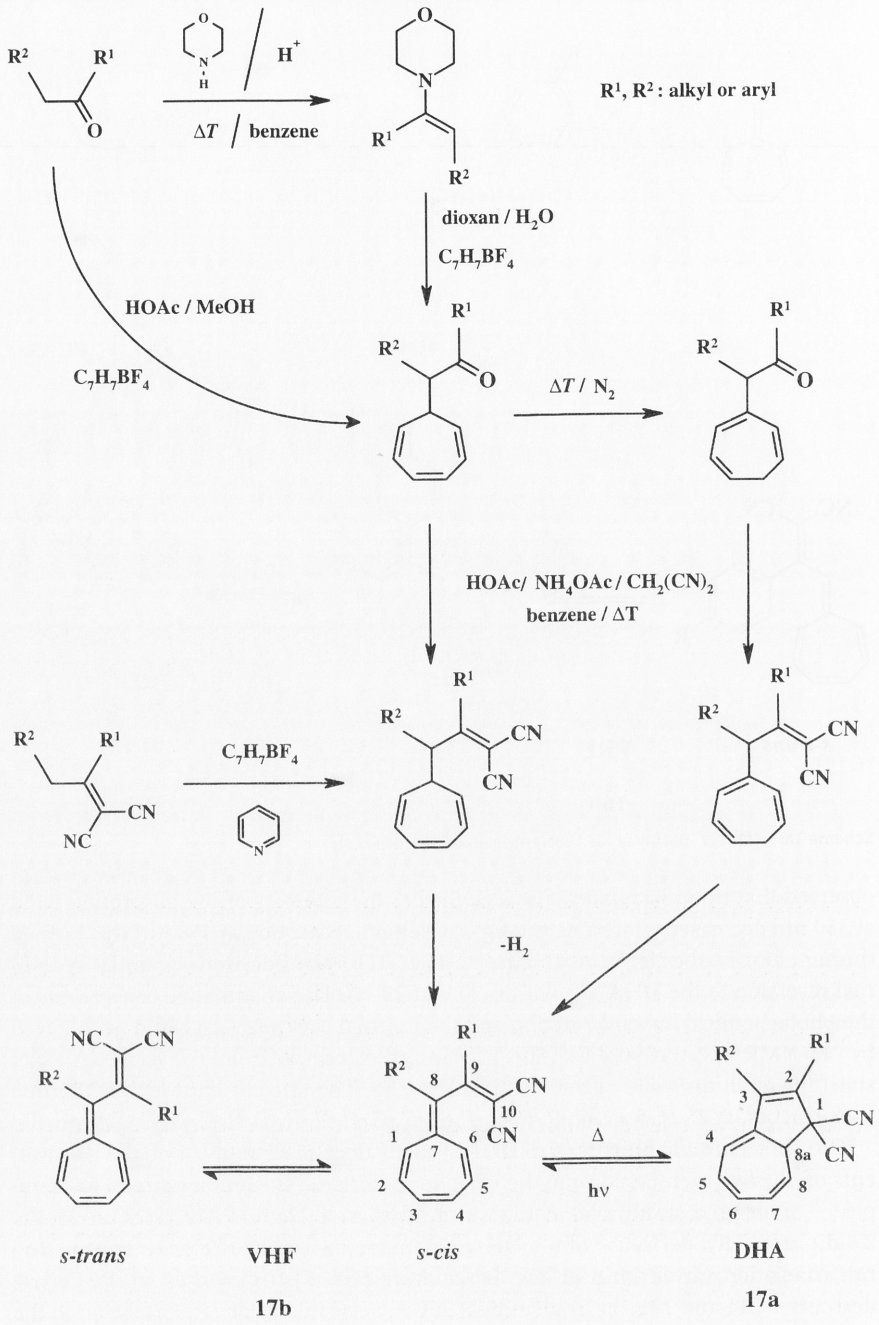

Scheme 1b: Synthesis of dihydroazulenes via corresponding vinylheptafulvenes; ΔT = reflux.

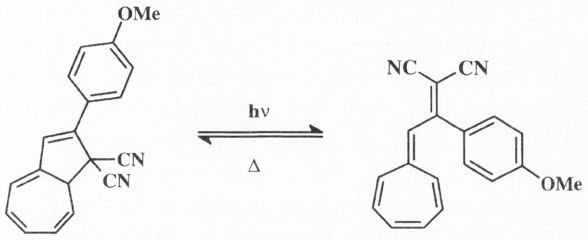

DHA **VHF**

18a **18b**

Scheme 2: Photochromic isomerization between **18a** and **18b**.

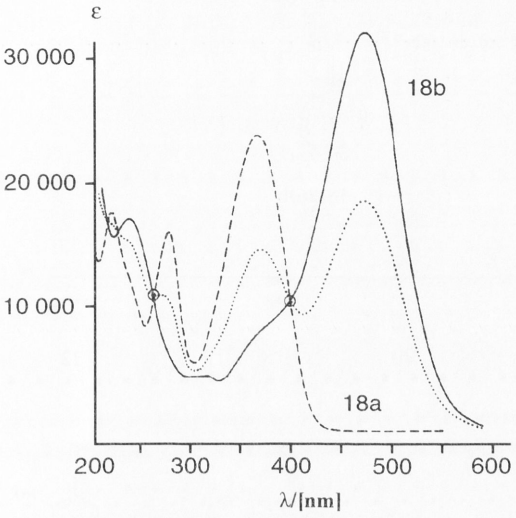

Fig. 9: Photochemistry of **18a** in acetonitrile ($c = 4.9 \times 10^{-5}$ mol dm^{-3}), irradiation by sunlight. (---) start; (•••) after 1 min, (—) after 7 min.

ents such as nitro and cyano groups facilitate the thermal back reaction. On the other hand, electron-donating substituents such as amino groups have the opposite effect.

The effect of substitution patterns on the long wavelength absorptions of various **DHA**s and **VHF**s are clear from Table 1.[21] The tricyanovinyl-substituted system **20a/20b** differs significantly (Figure 10), **DHA 20a** absorbing at 450 nm (in DMSO) and **VHF 20b** at 610 nm. This can be explained by charge transfer transitions due to the strong acceptor group. In addition, the shoulder on the absorption band of **20b** is aberrant. We explain this by the presence of both s-*trans* and s-*cis* forms in solution.[21c]

A furan substituent at the C-2 position in a **DHA** has a significant effect on the kinetics of the photochemical and thermal reactions, as illustrated for the case of the **DHA 19a** (Scheme 4). In this case, to observe the photochemical formation of the **VHF 19b**, the system must be cooled down to –50 °C, due to the fast thermal back reaction.

Another significant observation is that the photochemical ring-opening of the **DHA 18a** to the corresponding **VHF** is blocked in the crystalline state; this is probably due to the crystal packing. Irradiation of **DHA 18a** in poly(methyl methacrylate) film, however, results in the formation of **VHF 18b** (Figure 11). On heating at 80 °C, it reverts quantitatively to **18a**. This observation reinforces speculation that crystal packing plays a major role in the photochromic behavior of **DHA 18a**.

Attachment of **DHA 26a** to cellulose, as a biopolymer representative, provides another way to test the feasibility of multifold photochromic switching within a

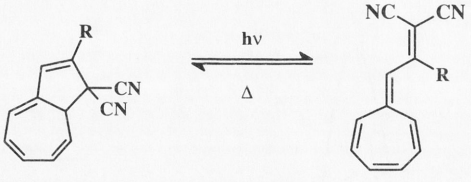

(18-26)a **(18-26)b**

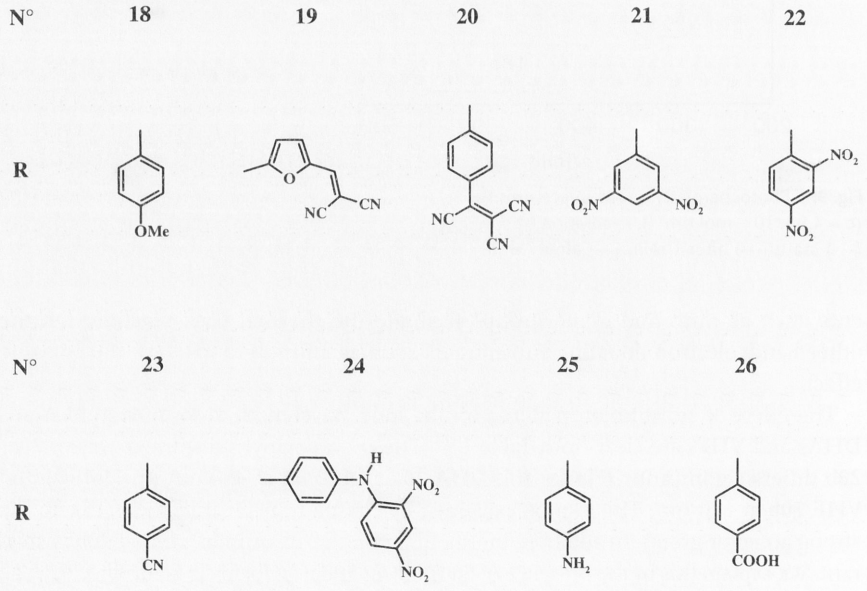

Scheme 3: Various **DHA-VHF** couple substitution patterns.

Tab. 1: Absorption maxima of **DHA**s and **VHF**s and quantum yields $\phi_{DHA \rightarrow VHF}$ of **DHA→VHF** photoreactions in nondegassed solutions at 24 °C, $\lambda_{irr} = 366$ nm. (a) At −50 °C, $\lambda_{irr} = 420–480$ nm; (b) At 25 °C; absorption at 608 nm assigned to *s-trans*-**VHF**; absorption at 680 nm assigned to *s-cis*-**VHF**; (c) Same value in argon-saturated solution; (d) Limiting value due to thermal back conversion.

Compound	*Solvent*	λ_{DHA} *[nm] (a)*	λ_{VHF} *[nm](b)*	$\phi_{DHA \rightarrow VHF}$
2-Phenyl-DHA	methylcyclohexane	349	440	0.35
	toluene	354	459	0.6
	ethanol	348	468	0.5
	acetonitrile	350	468	0.55
18	acetonitrile	360	465	0.4
19	ethanol[a]	440	548	
20	DMSO	449	608, 680 (sh) [b]	
21	methylcyclohexane	362	464	0.55
	toluene	368	482	0.45[c]
	ethanol	364	492	0.09
	acetonitrile	364	490	0.002[c]
22	toluene	310	480	0.005
	ethanol	315	470	≤ 0.008[d]
	acetonitrile	320	488	≤ 0.0004[d]
23	methylcyclohexane	361	452	0.4
	toluene	368	470	0.65
	ethanol	362	474	0.35
	acetonitrile	362	474	0.6
24	acetonitrile	386	468	
25	methylcyclohexane	376	440	0.4
	toluene	382	448	0.3
	acetonitrile	381	450	0.15
26	methylenechloride	361	474	

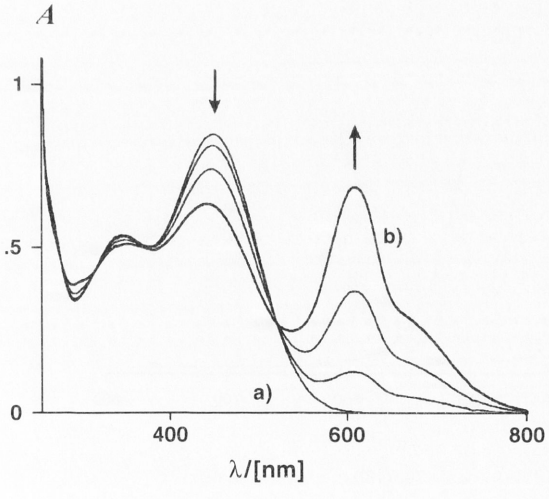

Fig. 10: Photochromism of **20a/20b** in DMSO (25 °C); irradiation with 366 nm light after 0 (a), 1, 5, 10 (b) seconds.

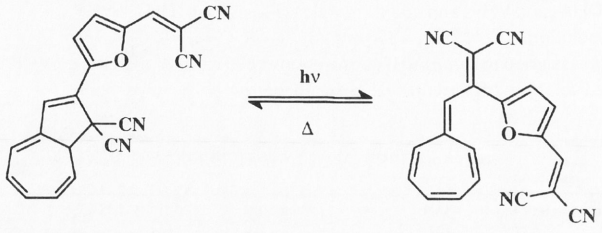

19a **19b**

Scheme 4: Photochromism of the furanyl-derivatized **DHA** derivative.

macromolecular architecture, as well as affording the opportunity to investigate the influence of the conformation of the polymeric network on photoswitching behavior.[22] Scheme 5 shows the photochemical conversion of the 6-*O*-[4-(1,1-dicyano-1,8a-dihydroazulen-2-yl)-benzoyl]-2,3-di-*O*-methylcellulose **27a** (degree of substitution of the photochromic subunit equals 0.25). Irradiation of a solution of **27a** in THF caused the characteristic **DHA** absorption band at 365 nm to decrease, while, on the other hand, the formation of the **VHF** derivative was verified by an increase in absorbance at 474 nm (Figure 12). After thermal relaxation, the original spectrum was restored. Note the blurred isobestic point at 400 nm, which we attribute to the structurally nonequivalent photochromic subunits.

Taking account of data from photophysical and photochemical investigations of the switching behavior of various **DHA/VHF** derivatives,[21,23] we assume a qualitative energetic profile of the **DHA/VHF** couple as depicted in Figure 13.

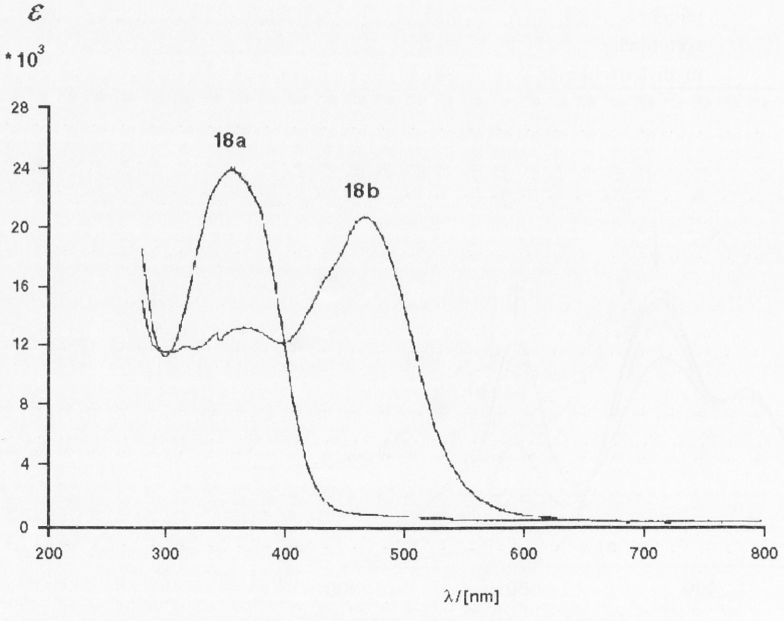

Fig. 11: Photochromism of the **DHA/VHF** couple **18a/18b** in a PMMA matrix.

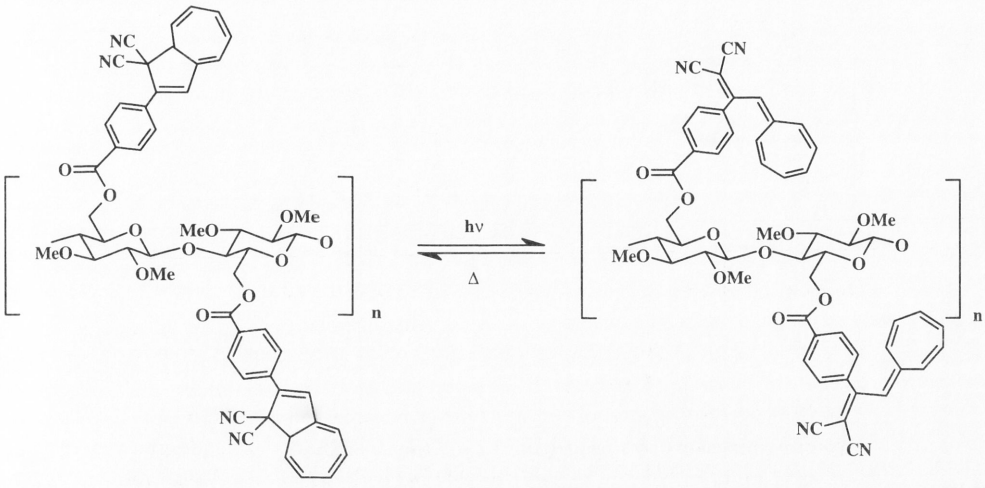

27a 27b

Scheme 5: Photochromism of **27a**.

DHAs undergo an efficient photoreaction to the corresponding **VHF**s; the quantum yields at room temperature ($\phi_{DHA \rightarrow VHF}$) range from very small values (≤ 0.0004) to a respectable 0.6 (Table 1). The **VHF**s are non-emitting and photochemically inactive. X-ray analytical investigations of crystallized photoproducts have revealed the exclusive formation in the crystalline phase of the *s-trans* **VHF** isomer.[19a] In solution, where a thermal equilibrium exists between the *s-trans* and *s-cis* isomers, we assume a high concentration of the thermodynamically favorable *s-trans*

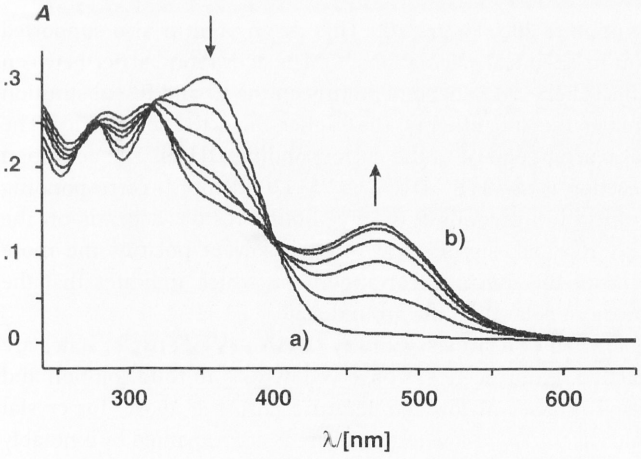

Fig. 12: Spectral developments on irradiation of **27a** in THF with an Osram 500 W lamp: 0 s (a), 200 s (b).

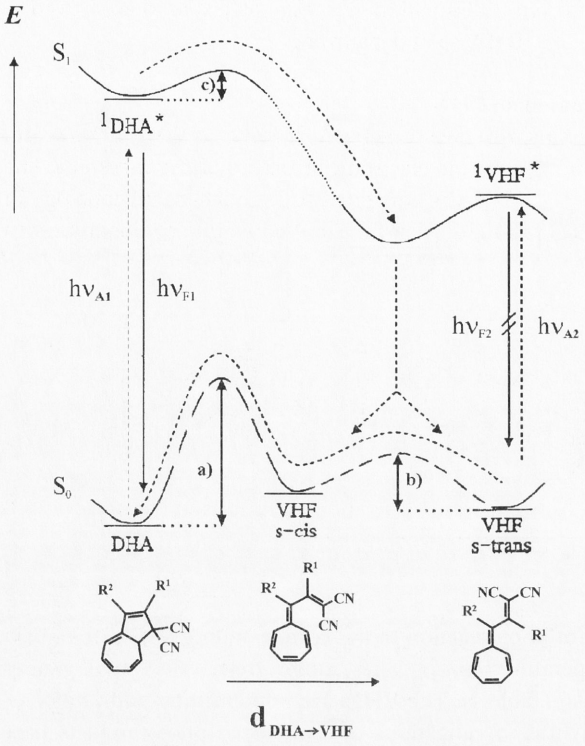

Fig. 13: Schematic representation of the reaction profiles of the photochemical pathway **DHA→VHF** and the thermal pathway **VHF→DHA**. Thermal barriers a), b), and c) are dependent on solvent parameters and substitution pattern. Absorption: $h\nu_{A1}$, $h\nu_{A2}$. Fluorescence: $h\nu_{F1}$, $h\nu_{F2}$ ($h\nu_{F2}$ is not detected).

form (see, however, compound **20b**, Figure 10). This assumption is also supported by semiempirical quantum chemical calculations.[24] The activation barrier between the *s-trans* and *s-cis* forms is believed to depend mainly on the R^1 and R^2 substitution pattern: that is, the bulkier the substituents, the higher the activation barrier. The **VHF**s undergo thermal rearrangement to the corresponding **DHA**s. The activation barrier for this back reaction (*s-cis*-**VHF→DHA**) is 75–110 kJ mol^{-1}, corresponding to half-lifes ranging from a few seconds to several hours. It, too, depends on the substitution pattern (R^1, R^2) and, significantly, on the solvent polarity: the more polar the solvent, the faster the thermal rearrangement, which indicates that the transition state must be more polar than the ground state.

The photoproduct is formed by a singlet pathway ^{1}**DHA*****→VHF**; triplet states are not involved in this reaction. Fluorescence is observed, weakly in fluid solution and with greatest efficiency in glasses at low temperature (also see above, for crystal packing effects). The increase in ϕ_F at low temperature is accompanied by a notably retarded **DHA→VHF** process, indicating competition between the photochemical

step ($\Phi_{DHA \rightarrow VHF}$) and photophysical dissipation of energy (ϕ_F), due to an activation barrier (< 21 kJ mol^{-1}) along the $^1DHA^* \rightarrow VHF$ pathway.

3.2.4.1 Molecular Switches Based on DHA-VHF

The photochemical ring-opening reaction of a **DHA**, leading to the colored **VHF**, brings about considerable changes in the electronic structure of the π-system. The alternant conjugated π-system in **DHA** is converted to a nonalternant topology in **VHF**. During this process, the cyano groups of the **DHA** come into conjugation with

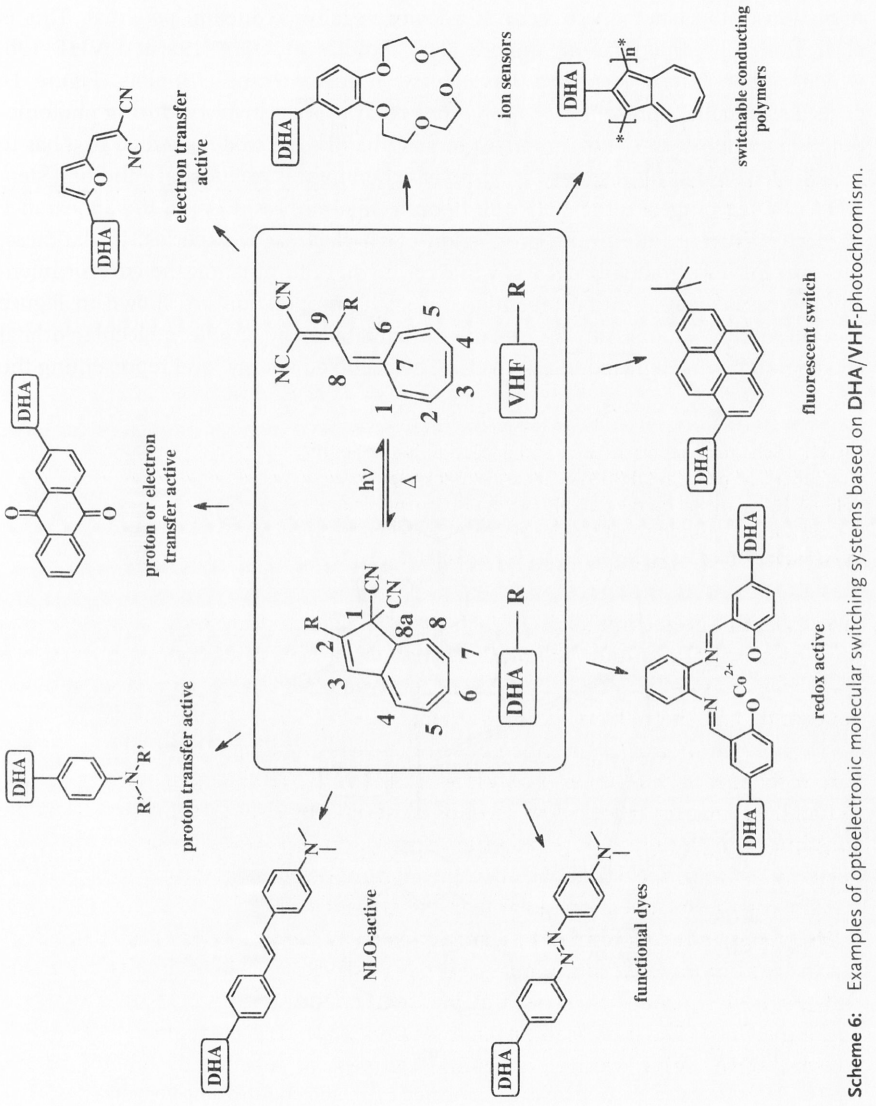

Scheme 6: Examples of optoelectronic molecular switching systems based on **DHA/VHF**-photochromism.

the π-system of the **VHF**, which strongly influences the electronic properties of the substituent at C-9. This versatile photochromic rearrangement can therefore allow photoswitching of electronic properties such as fluorescence, redox potentials, and optical nonlinearity, leading to a variety of optoelectronic molecular switching systems,[25] as illustrated in Scheme 6.

The furan-derived **DHA 19a** is an interesting photochromic system from the point of view of molecular switch development.[26] This system consists of a photochromic **DHA** structure and an electron transfer active dicyanovinylfuryl group. Since the electron acceptor strength of the dicyanovinylfuran is increased upon the photochemical rearrangement of the **DHA 19a** to the **VHF 19b**, the electrochemical reduction of the latter must occur at a lower negative reduction potential. This is clear from photomodulation amperometric studies of **DHA 19a** and **VHF 19b**, which demonstrate a structure dependency in current/time (*I*/*t*)-plots. Figure 14 gives a schematic representation of the molecular process involved during photomodulation amperometry. It is important to note that the electrode potential first has to be adjusted so that no response is observed when light is excluded. In the first step, **DHA 19a** rearranges to the **VHF 19b** upon irradiation, resulting in the appearance of electric current, due to the production of an electroactive species. In darkness, this current flow gradually decays, while on further illumination the current intensity increases again. Several repetitions of such an operation are shown in Figure 15. These observations can be explained qualitatively by simple molecular orbital considerations, as depicted in Figure 16. The occupied energy level representing the

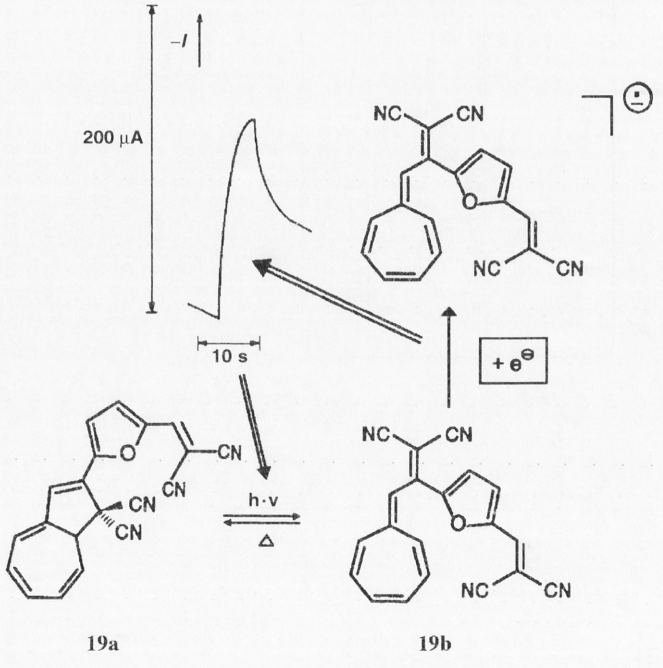

Fig. 14: Light-triggered electron transfer, monitored by photomodulated amperometry.

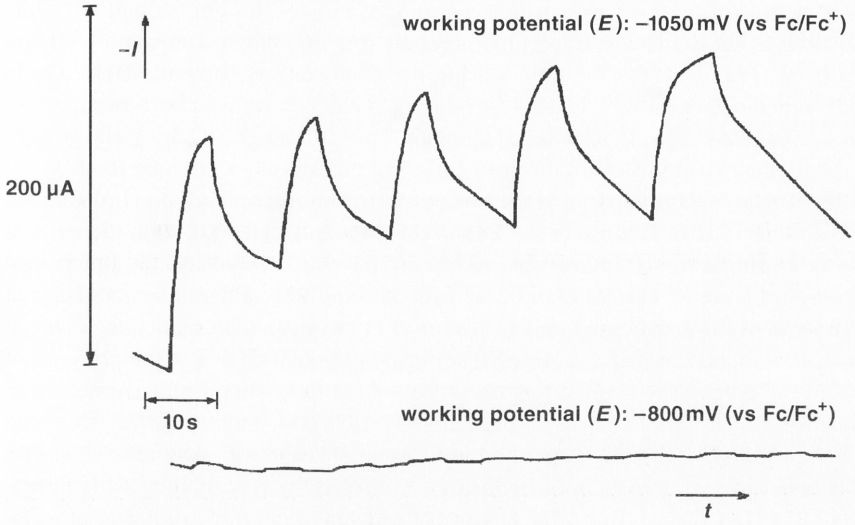

Fig. 15: Upper plot: Photostimulated electron transfer activation induced by irradiation of **DHA 19a** in acetonitrile ($c = 10^{-3}$ mol dm^{-3}) at working potential –1050 mV vs. Fc/Fc^+. Lower plot: No switching occurred at working potential –800 mV vs. Fc/Fc^+.

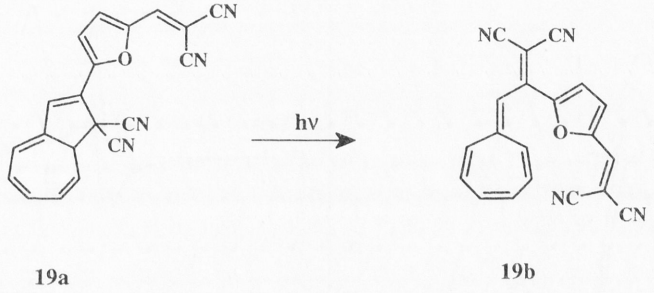

19a **19b**

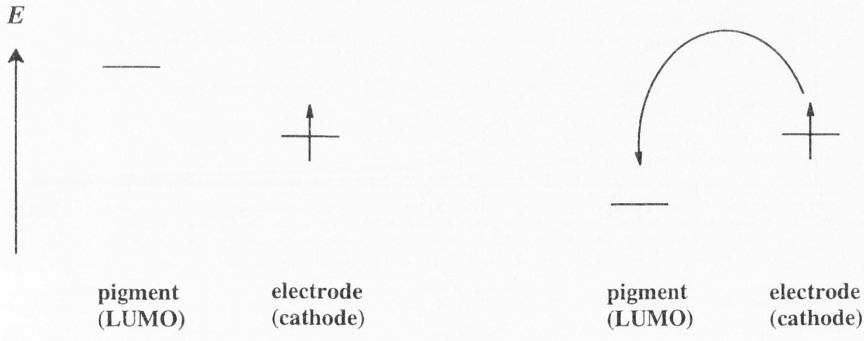

Fig. 16: Schematic representation of electronic changes due to photostimulated electron transfer.

cathodic electrode potential is maintained constant under this approximation, while the energies of the lowest unoccupied orbitals (LUMO) of the **DHA** and **VHF** are structure-dependent. For example, during the photoconversion of the **DHA 19a** to **VHF 19b**, the energy of the LUMO decreases and electron transfer becomes thermodynamically favorable, as shown in Figure 16. This process of switching allows light pulse inputs to be translated into electrical signal outputs at a molecular level.

The cyclic voltammetry, UV/Vis spectroelectrochemistry, and photomodulated amperometry characteristics of the **DHAs (21–24)a** and **VHFs (21–24)b** (Scheme 3) are quite interesting.[20] Reversible reduction waves were noticed for the radical anion formation of **21a**, **22a**, and **24a**, with **21a** and **22a** undergoing reduction at comparatively negative potentials (–1165 mV, –1130 mV). The reduction waves of **24a**, however, occurred at a slightly higher negative potential, due to the presence of the amino group. The dianion formation turned out to be chemically irreversible in the case of **22a**, but supported a partially reversible **21a**, indicating **EC** (first step **e**lectron transfer, second step **c**hemical reaction) behavior. Absorption spectra obtained during electrochemical reduction confirmed the reversibility of the formation of **21a**$^{\bullet-}$ (492 nm) from **21a** (Figure 17) and **22a**$^{\bullet-}$ (559 nm) from **22a**, observations consistent with dinitrophenyl radical anions. Cyclic voltammograms measured after stepwise "off-line" irradiation of **23a** in homogeneous solution are shown in

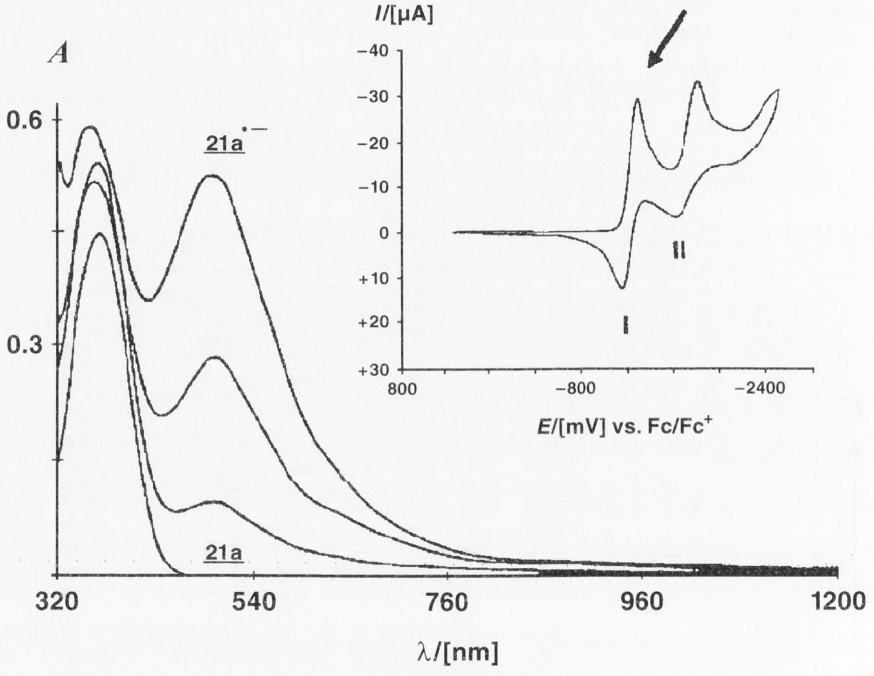

Fig. 17: Spectroelectrochemistry of **21a**, formation of the radical anion **21a**$^{\bullet-}$ on application of –900 mV (vs. Ag/AgCl). Inset: Cyclic voltammogram of **21a** in acetonitrile with 0.1 mol dm^{-3} TBAHFP, at a Pt electrode vs. Fc/Fc^{+} and a scan rate of 50 mV s^{-1}.

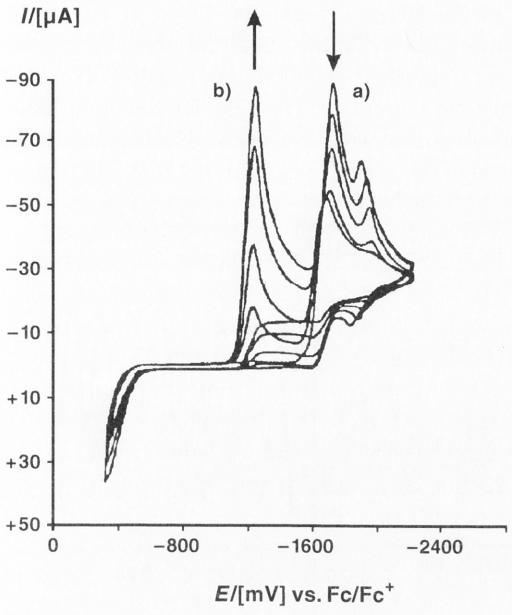

Fig. 18: Cyclic voltammogram of **23a** after irradiation (under nitrogen); irradiation time (in min): 0 (a), 2, 4, 8, 12 (b). Irradiation was performed using an Osram HWLS 500 W lamp as the light source.

Figure 18. On irradiation, a new peak appears, indicating the formation of a new species with a less negative reduction potential. After irradiation for 16 min, **23a** showed a distinctly different *I*/*E* trace, as shown in Figure 19. This observation indicates that the **VHF** form **23b** is reduced at a less negative potential, due to its π-acceptor dicyanovinyl substituent.

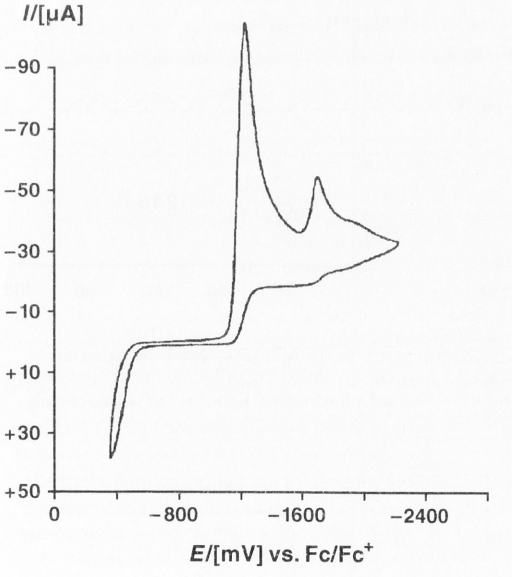

Fig. 19: Cyclic voltammetry of **23a** after irradiation for 16 min. Same conditions as Figure 18.

Photomodulation amperometry of the **DHAs (21–24)a** is shown in Figure 20. Because of the increased acceptor strength in **22b**, the 2,4-dinitrophenyl derivative **22a** exhibits oscillating behavior at an electrode potential less negative than that required for the constitutional isomer **21a** (Figure 20: **21a**, **22a**). On the other hand, the 4-cyanophenyl derivative **23a** displays increased sensitivity, which seems to be the result of the higher quantum yield of the photoreaction from **23a** to **23b** (Figure

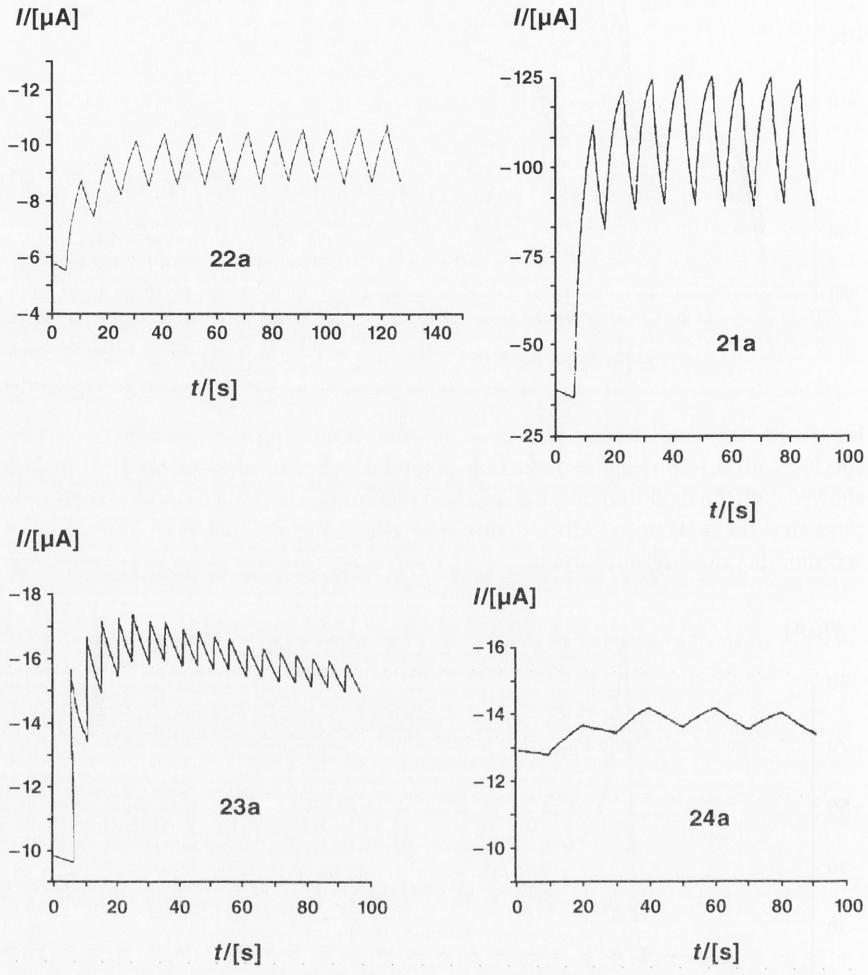

Fig. 20: Current changes produced by **21a**, **22a**, **23a**, and **24a**, respectively, upon irradiation in acetonitrile ($c = 5.9 \times 10^{-4}$ mol dm^{-3} (**21a**), 9.9×10^{-4} mol dm^{-3} (**22a**), 8.9×10^{-4} mol dm^{-3} (**23a**), 8.8×10^{-4} mol dm^{-3} (**24a**)). The "ON/OFF" switching times, in seconds, are: **21a**, 5/5; **22a**, 5/5; **23a**, 0.25/5, and **24a**, 10/10 at working potentials of –700 mV, –500mV, –900 mV, and –500 mV, respectively. Undivided electrochemical cell with optically transparent working electrode (OTE) [indium oxide/tin oxide (ITO) on glass] also serving as the window for irradiation; counter electrode glassy carbon, quasi-reference electrode Ag/AgCl; light source 1000 W Xenon-Mercury arc lamp LXM 1000–1 (Conrad-Hanovia).

20: **23a**). Finally, the effect of π-conjugation is demonstrated by bisarylamine **24a**, the poor sensitivity (Figure 20: **24a**) of which is presumed to result from the decreased perturbation of the redox-active subunit by the photochemically induced valence isomerization. This results in a smaller difference between the reduction potentials of **24a** and **24b**.

Aryl-substituted **DHA**s **(21–24)a** are able to produce electric current flow as a consequence of photomodulation by means of a light pulse sequence. To be of practical use, the peak potential E_p of **(21–24)b** must be less negative than the E_p of **(21–24)a**. It has been demonstrated that various factors can improve the sensitivity of the oscillating behavior. For example, high photochemical reaction quantum yields, reduction at less negative electrode potential, and a strong interaction between the acceptor subunit and the **VHF** moiety (leading to enhanced stability of the radical anions of **(21–24)b**) all exert significant influence on the oscillatory behavior. Photomodulation of these compounds enables an electric current to be triggered by light pulses.

The photochromic properties of the ferrocene-dihydroazulene conjugate **28a** are dependent on the oxidation state, making the compound a novel, redox-active photochromic molecular switching unit.[27] It is interesting to note that irradiation of compound **28a** with visible light at room temperature did not show any evidence for its ring-opening to the **VHF 28b** (Scheme 7). This could be the result of the fast thermal back reaction, or may be due to quenching by the auxiliary ferrocene moiety. On the

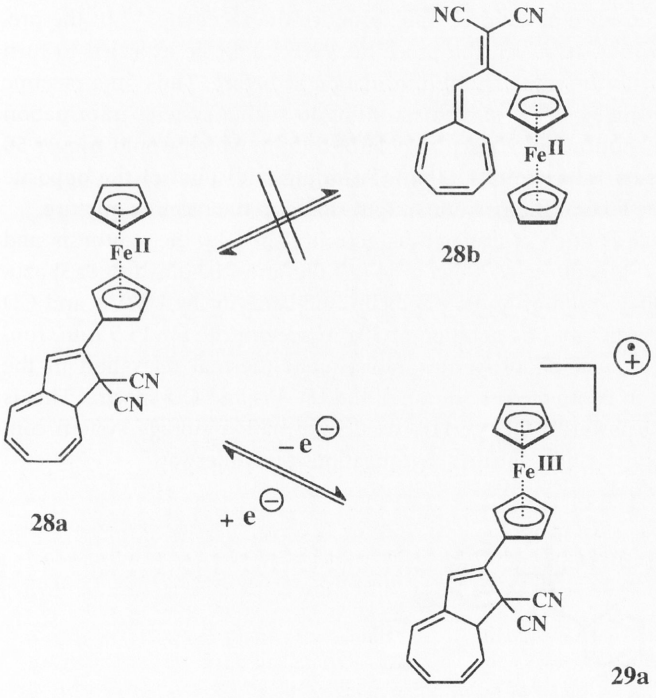

Scheme 7: Electrochemical triggering of photochromism.

other hand, the oxidized form **29a**, when irradiated with visible light, showed the long wavelength absorption corresponding to the vinylheptafulvene moiety (λ_{max} = 470 nm), while the absorption due to the dihydroazulene chromophore at 362 nm decreased significantly.

Photochemical reactions influenced by chiral auxiliaries represent another interesting aspect of molecular switches and optical data storage systems.[16,28] For purposes of manipulating photochemical reactions in a desired stereochemical sense, it is necessary to consider two different cases:[29] *asymmetric photochemistry* and the *photochemistry of chiral molecules*. The latter refers simply to the photochemistry of pure enantiomers, with no relationship to asymmetric induction. The former term, however, signifies photochemically induced transfer of optical information (by circular polarized light, for example) to a racemic substrate. This may be accomplished through the CD effect, which produces a difference in sensitivities between the enantiomers of a compound to left-polarized and right-polarized light. Consequently, it might be the case that only one enantiomer would be excited by light carrying specific chiral information. A fruitful combination of a photochromic compound with a distinct optically active moiety would give rise to an information storage system capable of storing twice as much information as one without a chiral attachment.

The chiral information intrinsic to the **DHA** system is vested in the asymmetric C-8a. In the case of the **DHA/VHF** couple, this information would be destroyed by the photochemical transformation into the prochiral **VHF**, since the thermal recyclization would, in the absence of a chiral 'flag', produce the racemate.[30] In the presence of a chiral auxiliary, however, the prochiral **VHF** might be expected to turn back into the **DHA**, with the same chiral information as before. Thus, in a racemic mixture consisting of molecules designed according to such a system, information could be read out by application of circular polarized light, which would trigger 50 % of the substrate (first information output). Scanning with light of the opposite polarity would give the second information output stored in the racemic mixture.

One approach towards such a system was accomplished by the synthesis and examination of (*S*)-1,1′-binaphthyl-2,2′-diyl bis[4-(1,1-dicyano-1,8a-dihydro-(8a*S*)-azulen-2-yl)]-benzoate (**30a**), monitoring its photochromic behavior by UV/Vis and CD spectroscopy. After irradiation of a solution of **30a** in acetonitrile for 15.5 min, fundamentally altering its spectral properties, subsequent thermal relaxation in the dark for 12h resulted in complete restoration of the UV/Vis and CD spectra. This is a first step towards a powerful **DHA/VHF**-based information storage system controlled by asymmetric induction. Further investigations are underway.

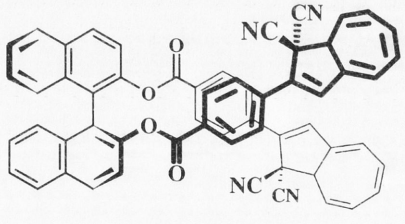

30a

3.2.4.2 Multimode Photochromic Switches Based on DHA-VHF

When covalently attached to electron transfer active subunits, the **DHA-VHF** couple can facilitate chemical and physical switching of electronic properties, as a result of photochemically induced rearrangement accompanied by a change in the redox potential. An interesting example of such a switching system is the compound containing a dihydroazulene component and a covalently attached anthraquinone moiety.[31] This system is able to act as a multimode switch, assisted by various processes such as photochromism, reversible electron transfer, and protonation-deprotonation reactions (Scheme 8).

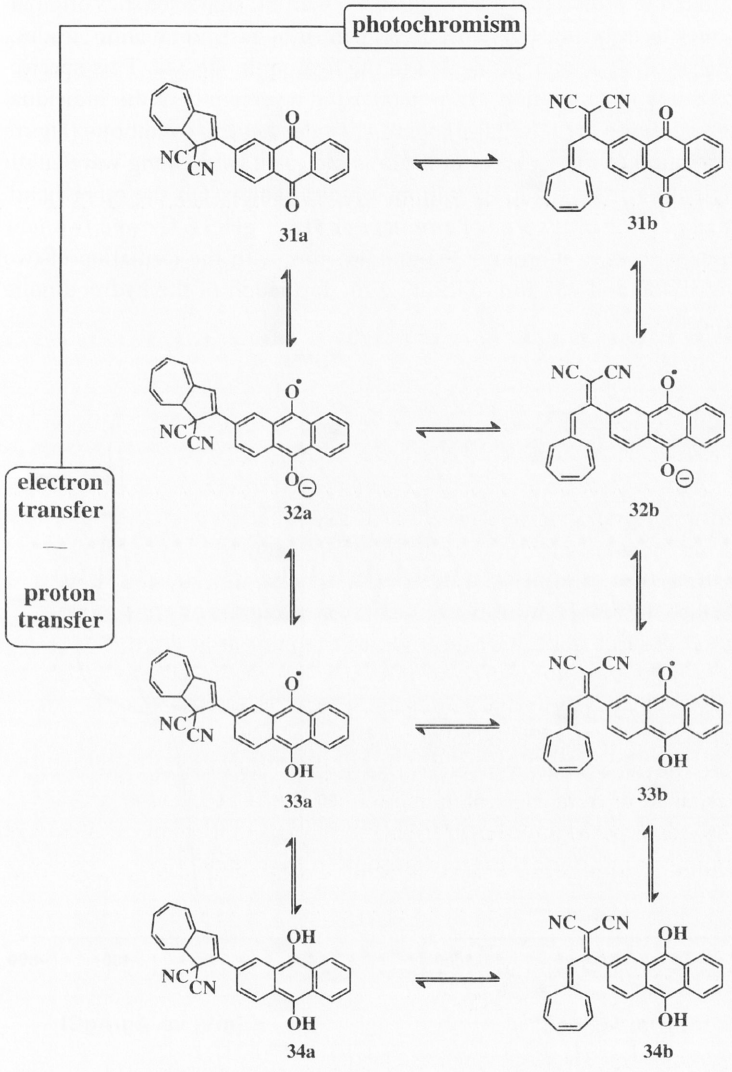

Scheme 8: Light-driven multimode molecular switching of the electron transfer active dihydroazulene **31a**.

The redox-active photochromic compound **31a** is reversibly reduced to the quinone radical anion ($E_{1/2}$ = –780 mV vs. Ag/AgCl) at a potential slightly less negative than that required for 9,10-anthraquinone ($E_{1/2}$ = –925 mV vs. Ag/AgCl) under the same conditions. The cyclic voltammogram of the anthraquinone **DHA** conjugate **31a** is shown in Figure 21. Further reduction of the radical anion to the dianion occurs irreversibly at $E_{1/2}$ = –1295 mV vs. Ag/AgCl at a scan rate of 250 mV, with the formation of a new species identified by an oxidation peak at Ep = + 90 mV vs. Ag/AgCl. The reduction of **31a** depends upon the solvent and pH. In tetramethylammonium acetate-acetic acid buffer, cyclic voltammetry of compound **31a** revealed a complex electron and proton transfer mechanism, with EC characteristics originating from two one-electron transfer steps, accompanied by fast protonation, leading through the intermediate semiquinone **33a** to the hydroquinone **34a**. This spectroelectrochemical study of compound **31a** reiterates the reversibility of the individual processes observed in the cyclic voltammograms. Under neutral conditions (Figure 22: top), the formation of the radical anion **32a** is indicated by the long wavelength absorption originating from the anthraquinone radical anion. On the other hand, the spectra obtained by multisweep voltammetry of **31a** at pH 5.6 showed two new absorption bands with λ_{max} at around 363 and 465 nm, with the formation of two isobestic points at 400 and 437 nm, indicating the formation of the hydroquinone **34a** (Figure 22/bottom).

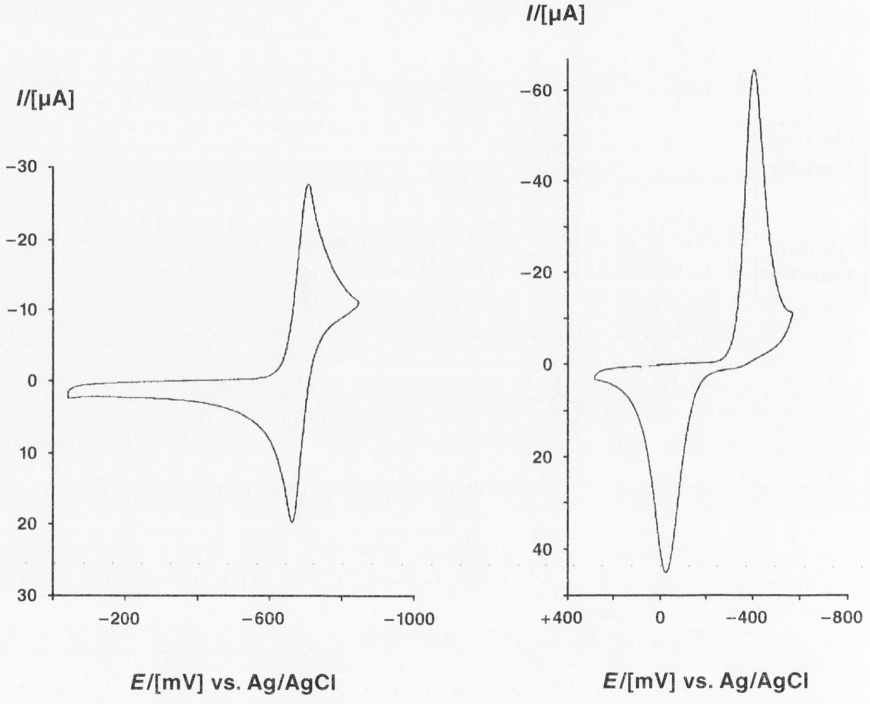

Fig. 21: Cyclic voltammetry of **31a** in acetonitrile as a function of pH. Left: under neutral conditions. Right: at pH 5.6 (ammonium acetate-acetic acid).

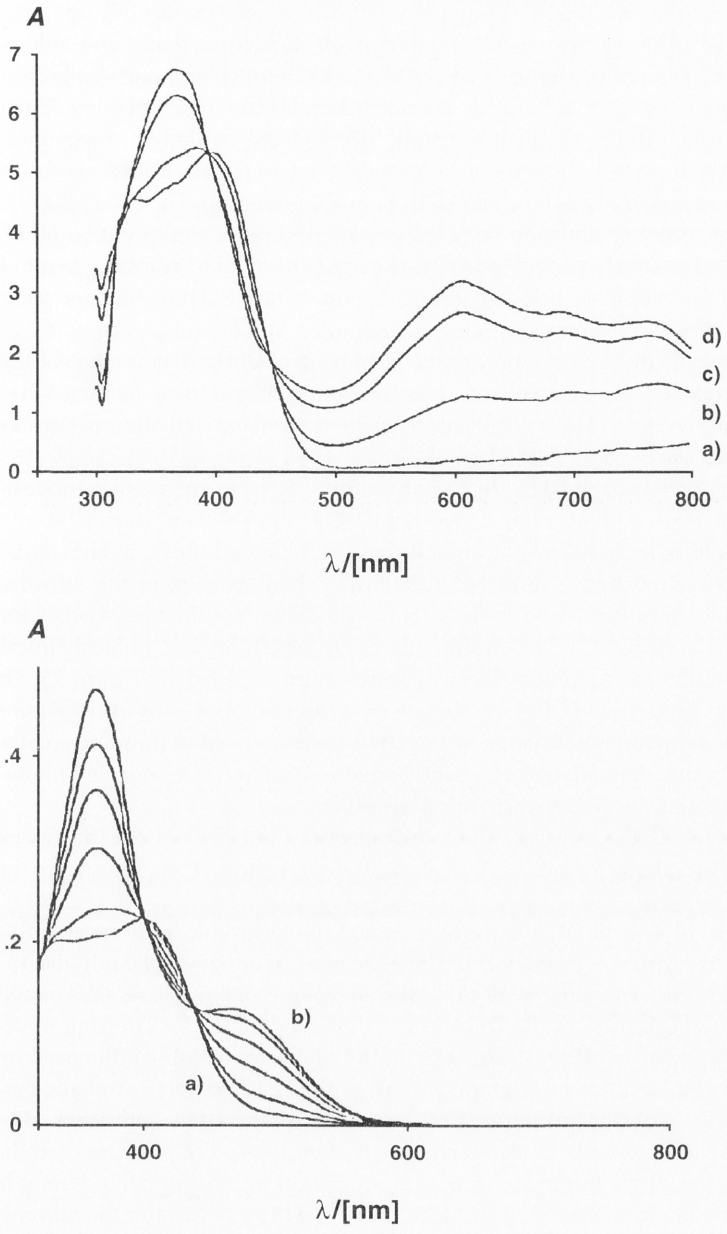

Fig. 22: Spectra obtained by multisweep voltammetry of **31a** as a function of pH. Top: in acetonitrile: (a) 0 mV, (b) –800 mV, (c) –900 mV, (d) –950 mV (vs. Ag/AgCl). Bottom: in acetonitrile at pH 5.6 (trimethylammonium acetate-acetic acid buffer): (a) 0 mV, (b) 700 mV (vs. Ag/AgCl).

It is interesting to note that the photochromic behavior of **31a** depends upon the solvent and the pH used during the irradiation. In dichloromethane and chloroform, the photochemical rearrangement of **31a** and its thermal back reaction is clear (Figure 23: top), whereas in acetonitrile the photochemical rearrangement could not be observed. Interestingly, the hydroquinone **34a** obtained by the electrochemical reduction of **31a** at pH 4–5 showed only a minor change in the absorption spectrum even after prolonged irradiation, as shown in Figure 23 (bottom). The switching signals obtained by photomodulation amperometry of a homogeneous solution of the anthraquinone **31a** are shown in Figure 24. During light-induced rearrangement of **31a** into **31b**, the reduction potential decreases and a fast electron transfer takes place, reducing **31b** to the corresponding radical anion and causing a cathodic current which retreats after interruption of the light source. Obviously, because of the fast electron transfer, even a small amount of the photochemically generated **VHF**-anthraquinone conjugate **31b** is sufficient to create the photomodulation pattern as shown in Figure 24.

Heteroaryl-functionalized **DHA-VHF** photochromic systems are another interesting class of multimode photochromic switches.[32] Electron-rich heteroaromatic subunits such as 1′-dibenzodioxinyl, 1′-thianthrenyl, 4′-phenoxathiinyl, 3′-phenothiazinyl, 3′-phenoxazinyl, and 2′-dimethylphenazinyl, when attached to the dihydroazulene chromophore, are found to be potential candidate multimode switches for information data storage[33]. The multimode redox switching and photochemical switching of electronic properties of such systems are depicted in Figure 25. In order to verify the viability of the multimode switching processes shown in Figure 25, a series of compounds consisting of the **DHA** system linked to those heteroaromatic subunits mentioned have been synthesized and subjected to detailed photochromic, redox, and spectroelectrochemical investigation.

The structures of the systems under investigation and the various processes involved in their photochemical and electrochemical switching are illustrated in Scheme 9.

Except for **DHA 40a**, all **DHA** derivatives exhibit photochromic behavior at ambient temperature, with the formation of the characteristic long wavelength absorption band of the corresponding **VHF (35–39)b**. As a representative case, the change in the absorption spectrum of the **DHA 37a** is shown in Figure 26. The long wavelength absorption bands of the **DHA**s were found to be considerably influenced by the donor strength and the substitution pattern of the attached heteroaromatic system, as we had noticed in earlier studies. For example, the **DHA** derivatives **(38–40)a**, which are less sterically hindered because of their C-2-C-3′{2′} linkages, exhibited bathochromic shifts in the absorption maxima with increasing donor strength of the heteroaromatic subunit. On the other hand, **DHA**s such as the thianthrene derivative **36a**, in which the heteroaromatic subunits are joined in the C-2-C-1′{4′}-fashion, showed significant hypsochromic shifts. Nevertheless, the absorption spectra of the corresponding **VHF**s are less dependent on the substituents at C-9.

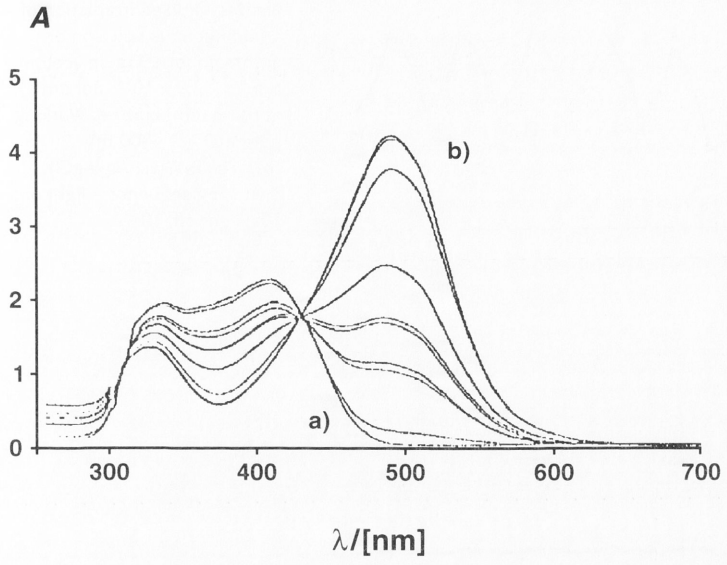

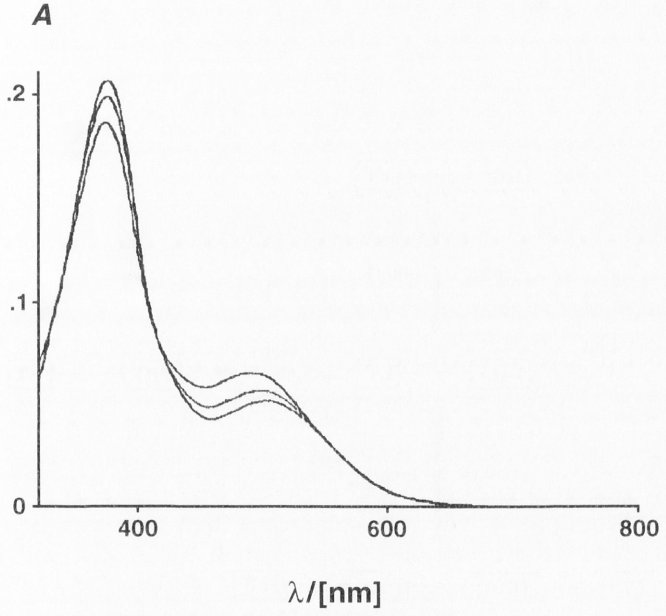

Fig. 23: Spectral changes upon irradiation of **31a**. Top: in dichloromethane, (a) before irradiation, (b) after 1 min irradiation with an Osram HWLS 500 W lamp. Bottom: in dichloromethane at pH 4–5, irradiation with a daylight lamp after reduction to hydroquinone **34a**.

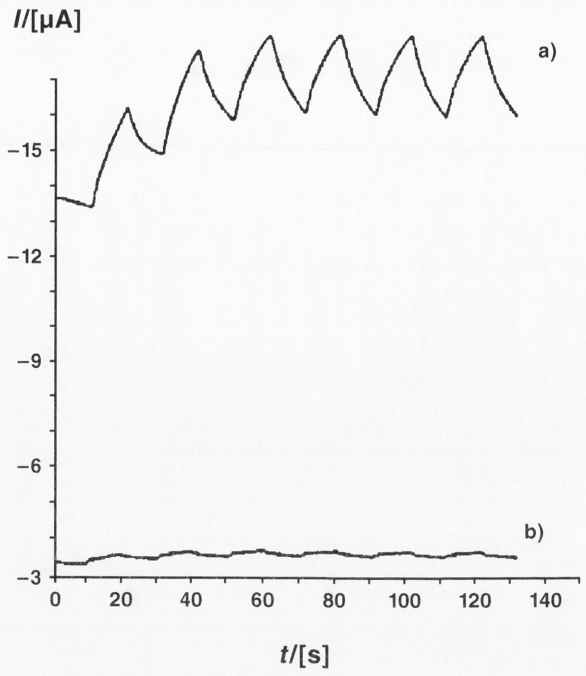

Fig. 24: Pulsed irradiation of a homogenous solution of anthraquinone **31a**, in acetonitrile ($c = 8.9 \times 10^{-4}$ mol dm^{-3}), at room temperature. Working potential: (a) –800 mV, (b) –700 mV (vs. Ag/AgCl). Switching sequence – light on: 10s, light off: 10s.

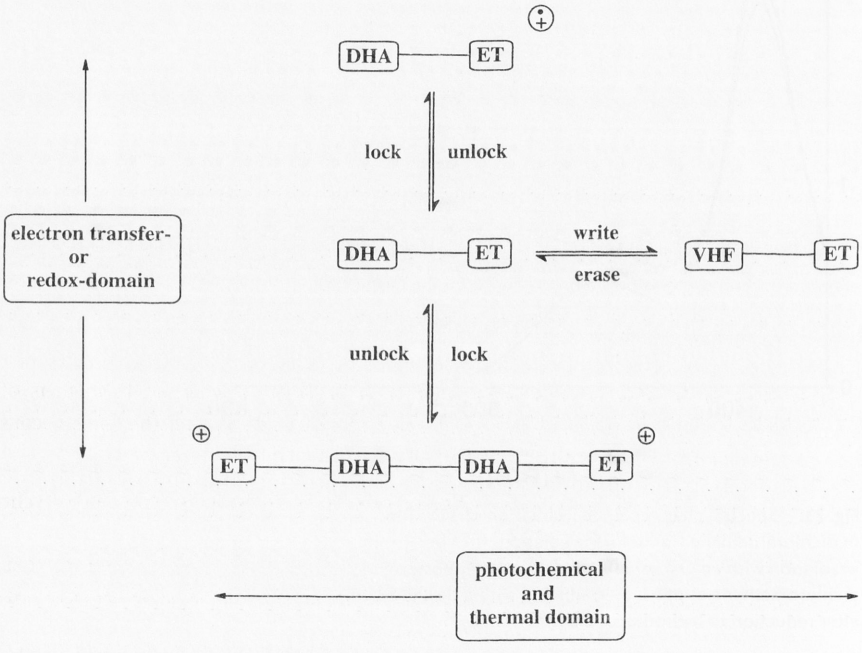

Fig. 25: Information storage in dihydroazulene/vinylheptafulvene systems attached to heteroaromatic groups.

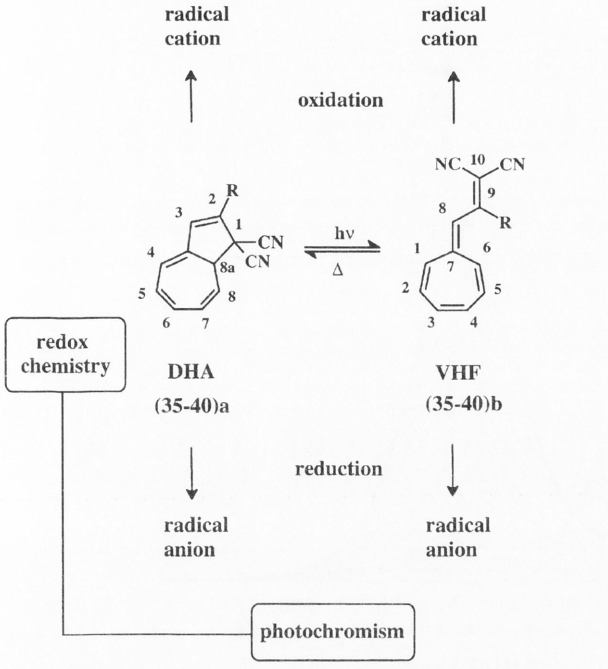

X = Y = O: 35
X = Y = S: 36
X = O, Y = S: 37

Z = S: 38
Z = O: 39
Z = N-Me : 40

Scheme 9: Photochromic and redox behavior of the **DHA/VHF** subunit, and the various heteroatomic groups used as substituents at C-2 of the five-membered ring.

Switching of the redox properties of **(35–40)a** has been examined by means of cyclic voltammetry and UV/Vis/NIR spectroelectrochemistry. For all **DHA-VHF** couples, we have observed three different I/E (current/potential) responses:

1) a reversible anodic wave ($E_{1/2}$ (het-ox)) for the oxidation of the heterocyclic structures of the **DHA** and **VHF** forms;
2) the waves (E_{pa} (ring-ox)/E_{pc} (ring-ox)), which signify the electrochemical oxidation (quasireversible or irreversible electrode process) of the dihydroazulene and vinylheptafulvene subunits, respectively;
3) the irreversible cathodic waves (E_{pc} (ring-red)) due to the reduction of the **DHA-VHF** subunits.

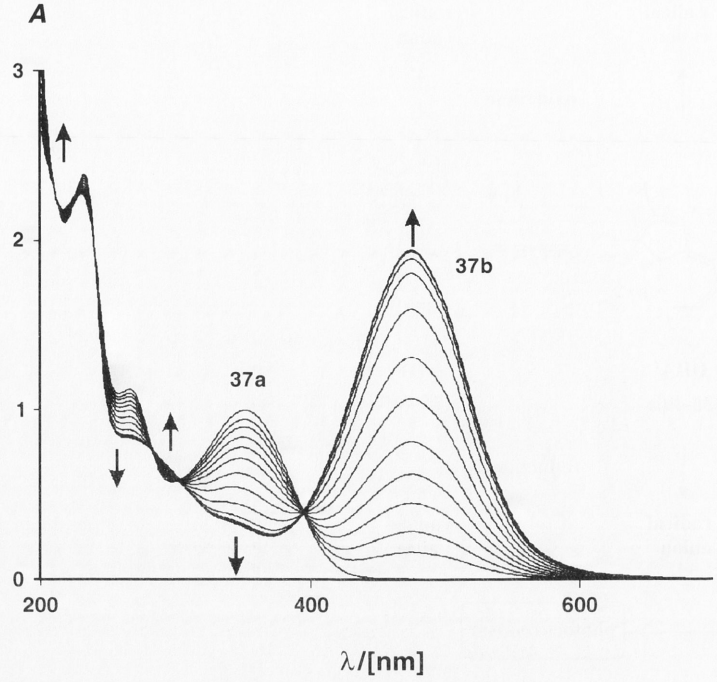

Fig. 26: Appearance of the long wavelength absorption of **VHF 37b** upon irradiation of **DHA 37a** in acetonitrile (20 °C, λ_{irr}: 260–390 nm).

The typical cyclic voltammograms of **DHA 35a**, before (unbroken line) and after (dashed line) irradiation (15 min) in daylight in acetonitrile, are shown in Figure 27. The broken line is assigned to the photoisomer **VHF 35b**, and is significantly different from that of the corresponding **DHA 35a**.

The thin layer cyclovoltammogram of **35a** showed two independent oxidation processes: (i) an irreversible wave at E_{pa} = 1034 mV (vs. Fc/Fc^+) (E_{pc} = –232 mV (vs. Fc/Fc^+)) and (ii) a reversible wave ($E_{1/2}$ (het-ox), which corresponds to the formation of the radical cation of the dibenzodioxin subunit (Figure 28). The irreversible wave represents a two-step process involving a one-electron oxidation of the **DHA** subunit followed by a chemical step (EC-type mechanism) leading to a significant change in the molecular structure. Since polyenic radical cations have a preference for dimerization,[34] it is reasonable to speculate on the formation of the dimeric dication species as shown in structure **41**. The chemical reversibility of this EC-type process was confirmed by multisweep thin layer experiments.

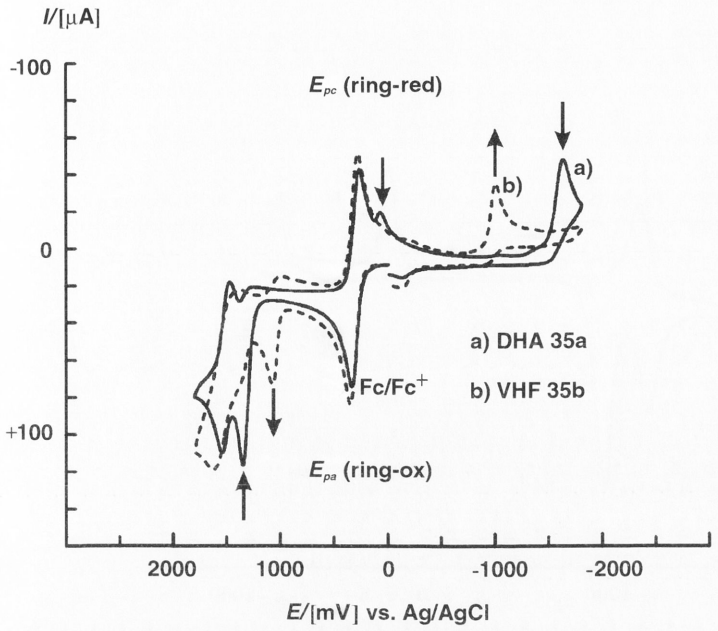

Fig. 27: Cyclic voltammogram of **DHA 35a** before (a) and after (b) irradiation (15 min) with daylight. Solvent: acetonitrile; ν = 250 mV s^{-1}.

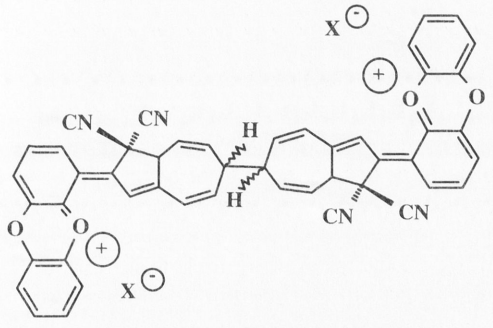

41

This interpretation of the irreversible oxidation wave (E_{pa} (ring-ox)) as being caused by the formation of the dimeric dication species **41** can be further substantiated by spectroelectrochemical studies. Figures 29 and 30 display spectroelectrograms for the first oxidation waves of the **DHA**s **35a** and **39a**. As foreseeable from the significantly different oxidation potentials, the features of the spectra are completely different, indicating varying regiochemistry in the oxidation processes. On electrochemical oxidation of the **DHA 35a**, the absorption of the neutral form at 353 nm decreases, while a strong band, too short to be attributable to the radical cation of **DHA 35a**, appears at 438 nm (Figure 29). In the case of **DHA 39a**, on the other hand, the long wavelength absorptions at 545 and 860 nm can be assigned to the

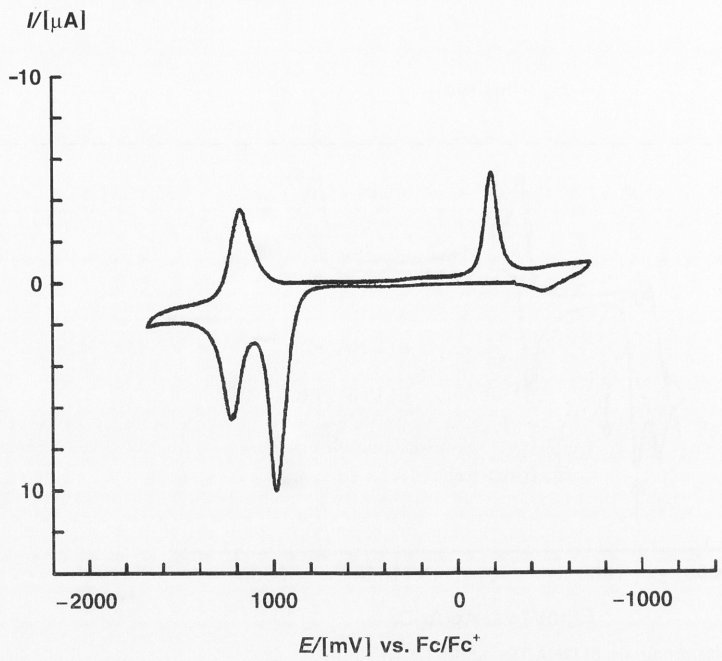

Fig. 28: Thin layer cyclic voltammogram of **DHA 35a** in acetonitrile; $\nu = 25$ mV s^{-1}.

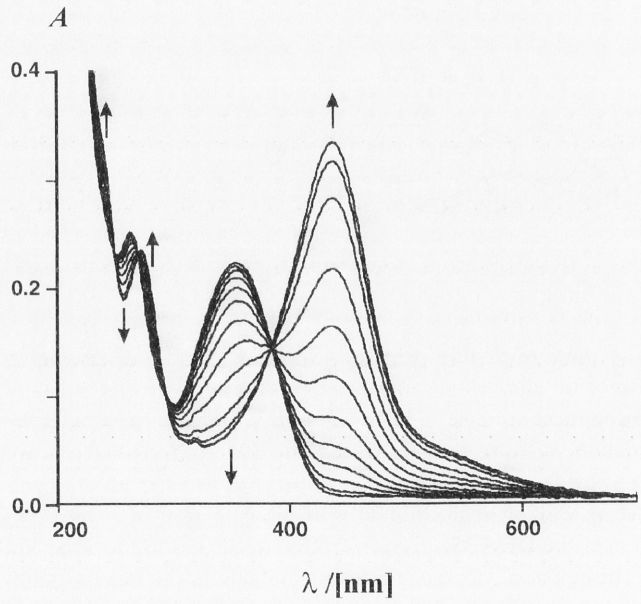

Fig. 29: Spectroelectrogram obtained on oxidation of **DHA 35a** to the dimeric dication **41** (solvent: acetonitrile).

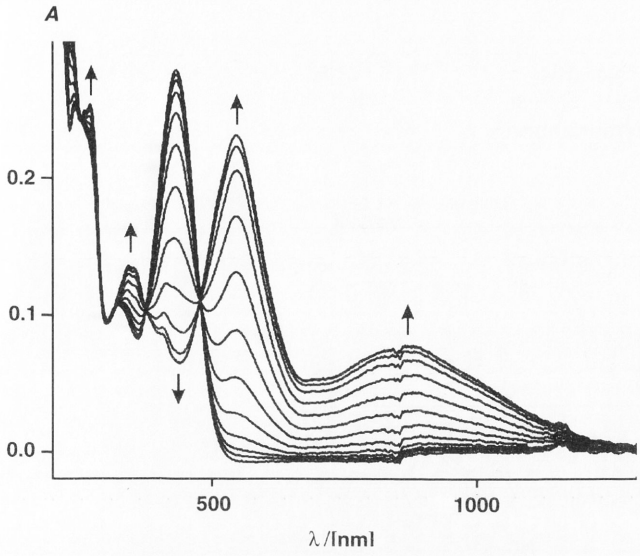

Fig. 30: Spectroelectrogram obtained on oxidation of **DHA 39a** to the radical cation **DHA 39a**$^{\bullet+}$ (solvent: acetonitrile).

radical cation (Figure 30). Thus, **DHA**s with weak donor substituents (**DHA (35–37)a**) undergo oxidative dimerization ('lock'-state), and such systems satisfy the requirements for application in information storage.

A strategy to enable multifold switching in macromolecular systems is briefly described below. On the basis of previous work, which showed that switchable and conducting films can be obtained by electropolymerization of 1,3-unsubstituted azulenes (Figure 31),[35] investigations were carried out on **DHA**/azulene derivatives.[36]

It was found that azulene derivative **42a** is non-photochromic at room temperature. The same was true for derivative **43a**. Obviously, if **DHA** and azulene subunits are strongly coupled, as in **42a** and **43a**, then photophysical deactivation processes must quench photochemical ring-opening. By careful screening of spacer-linked azulene/**DHA** conjugates, however, we found that amide-linked derivative **44a** clearly gave rise to ring-opening under photochemical conditions (Figure 32).

Monomer **44a** was also found to electropolymerize on indium-tin-oxide (ITO) under potential-sweep conditions (Figure 33). The resulting film (*poly*-**44a**) can be electrically doped by oxidation, as was demonstrated by UV/Vis spectroelectrochemistry (oxidative dotation leads to a broad absorption band beyond 1000 nm). We found that on irradiation with a 500 W incandescent lamp the pristine film (at 0 mV vs. Ag/AgCl) gave rise to the formation of the **VHF** form (*poly*-**44b**). Under thermal conditions, the **DHA** spectrum could be restored (Figure 34).

Recently, Diederich and co-workers have made use of the **DHA-VHF** system for designing a three-way chromophoric molecular switch, which can be controlled by pH, light, and heat.[37] The system is based on a molecule with three addressable subunits, that can undergo individual, reversible switching cycles. These processes

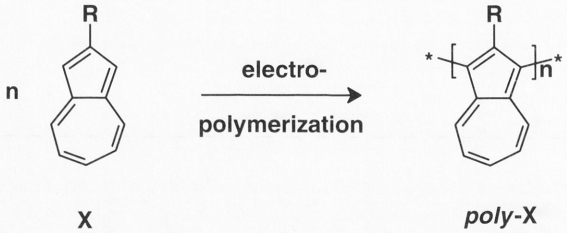

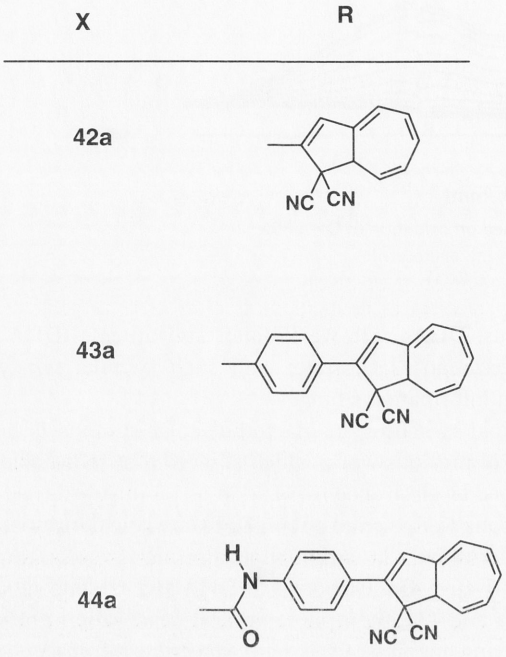

Fig. 31: **DHA/azulene** conjugates.

are illustrated in Scheme 10. With three possible switching processes, the molecule **45** can theoretically adopt eight interconvertible states, of which six states can be detected. Interestingly, the reversible conversions of *trans*-**45a** to *trans*-**45a**$^+$ and to *trans*-**45b**$^+$ function like an AND logic gate; the *trans*-**45b**$^+$ state can be obtained only in the presence of protons and light. In addition, three write/erase processes are also possible in system **45**: these are the reversible *cis–trans* photoisomerization between *trans*-**45a** and *cis*-**45a**, and the two reversible protonation/deprotonation processes of the *trans*-**45a**/*cis*-**45a** and *trans*-**45a**$^+$/*cis*-**45a**$^+$ couples. Since the fluorescence enhancement after deprotonation of **45a**$^+$ amounts to a factor of about 300, a very efficient, nondestructive information readout is available in the shape of the *cis*-**45a**/

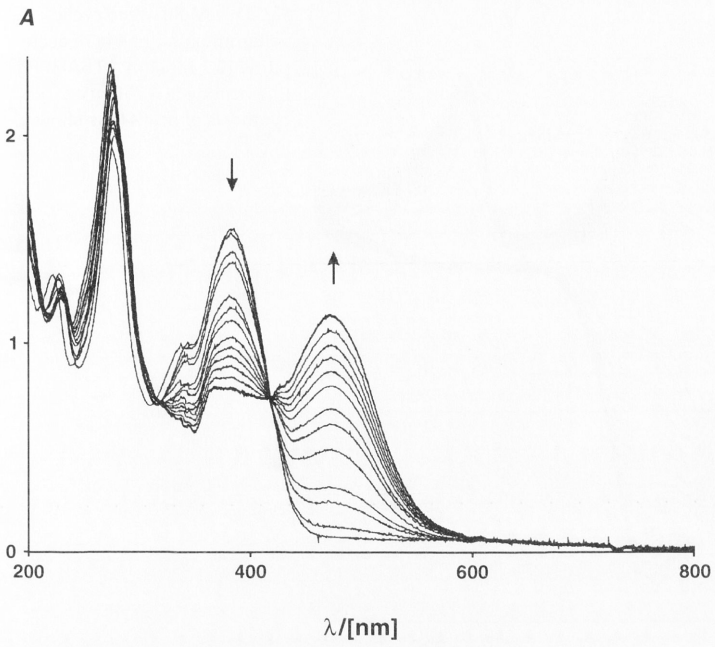

Fig. 32: Spectral changes on irradiation of **44a** (Hg/Xe lamp, Schott filter UG11, transmittance 250–390 nm) in acetonitrile ($c = 4.6 \times 10^{-5}$ mol dm^{-3}). Time of irradiation (seconds): 0, 5, 15, 25, 35, 45, 55, 75, 95, 110, 140, 200, 355.

45a$^+$ and *trans*-**45a**/**45a**$^+$ couples, at $\lambda_{\text{emission/ 45a}} = 606$ nm, by using excitation light of 396 nm for the *cis* isomer and 464 nm for the *trans* isomer.

In a recent development, the concept of multimode molecular switching in a cyclic four-stage process has been introduced in the form of a structurally fused photochromic system comprising a **DHA** component and a dithienylethene (**DTE**) moiety (Scheme 11)[38]. The open/open **47** and the closed/closed **48** are rapidly formed on irradiating the open/closed **46**. The open/open **47** rearranges thermally to **46**, whereas **48** can be made to revert to **46** photochemically. Figure 35 shows the spectral properties associated with these interconversions. This is the first attempt towards an electronically strongly coupled molecular switch, combining the **DHA-VHF** photochromic system with the well known dithienylethene system. In principle, this can give rise to four different switchable states: **46**, **47**, **48**, and **49**. However, the closed/open form **49** has not yet been observed in this system for the substitution pattern $R^1{=}R^2{=}CH_3$. It is expected that appropriate donor and acceptor groups at the dithienylethene moiety may facilitate its formation, and this is under investigation.

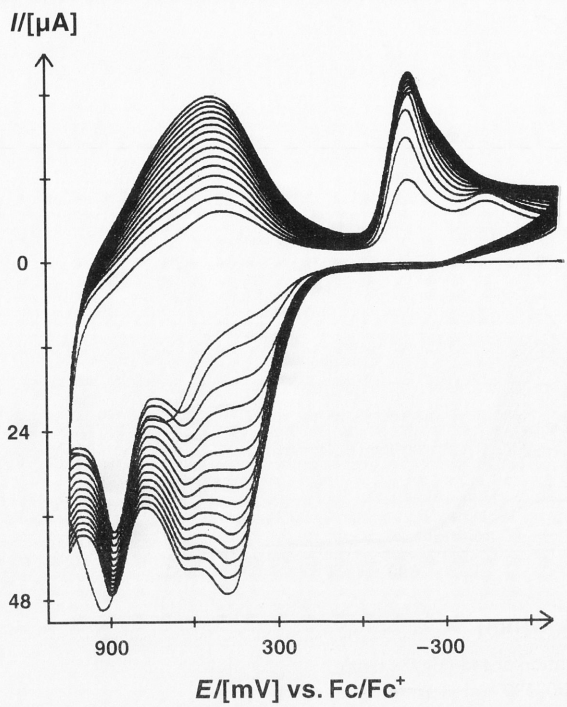

Fig. 33: Multisweep cyclic voltammogram of **44a** in acetonitrile (0.1 mol dm^{-3} TBAHFP, Pt electrode, $\nu = 250$ mV s^{-1}): Synthesis of *poly*-**44a** is shown.

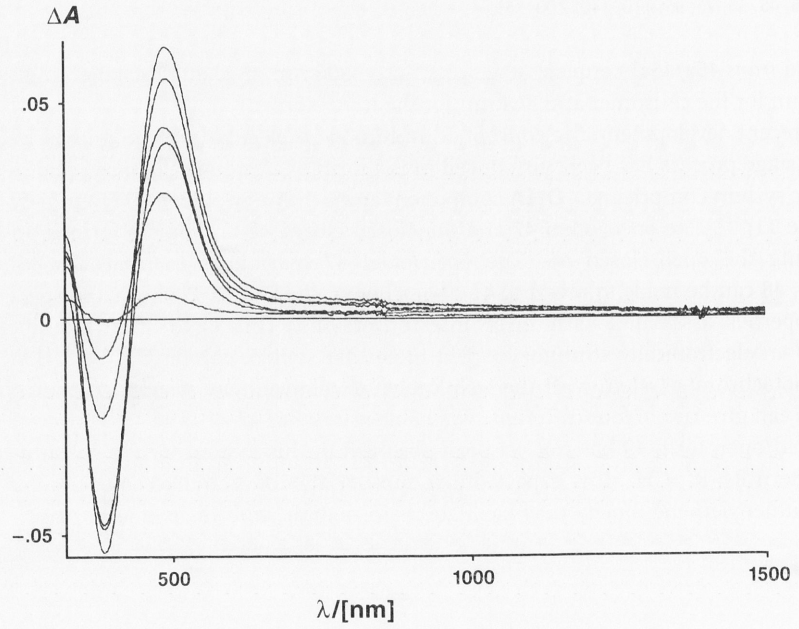

Fig. 34: UV/Vis/NIR difference spectra on irradiation of *poly*-**44a**. Irradiation times (min): 0, 4, 5, 7, 11, 16, 21.

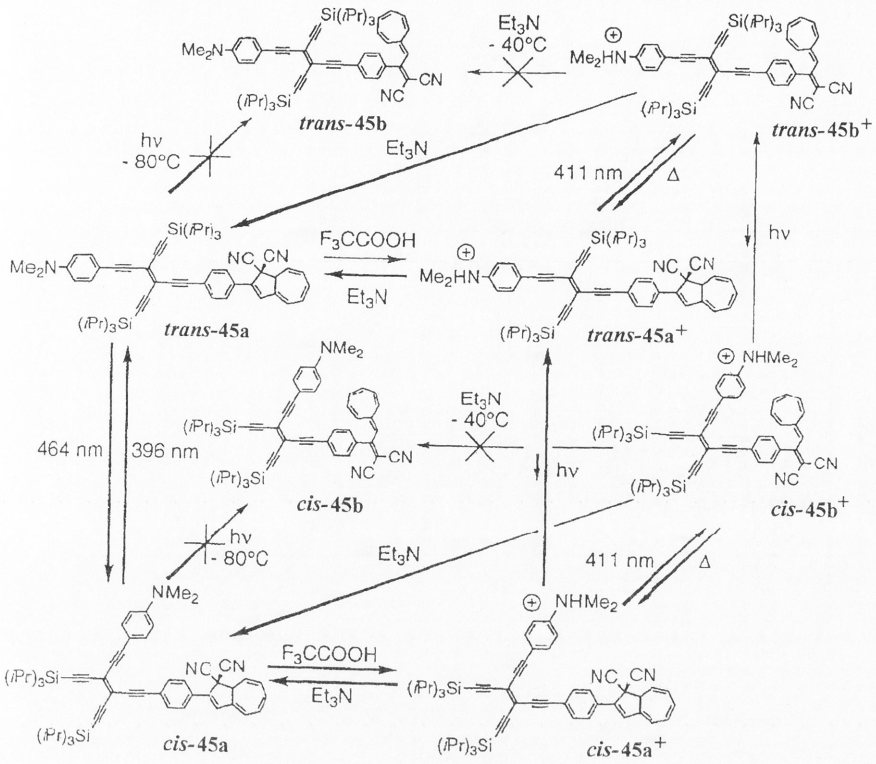

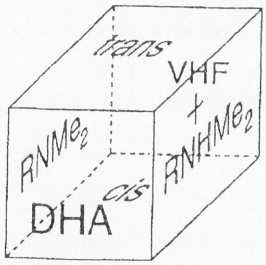

Scheme 10: Three-dimensional switching diagram of compound **45**. The eight possible states are shown as the corners of a cube.

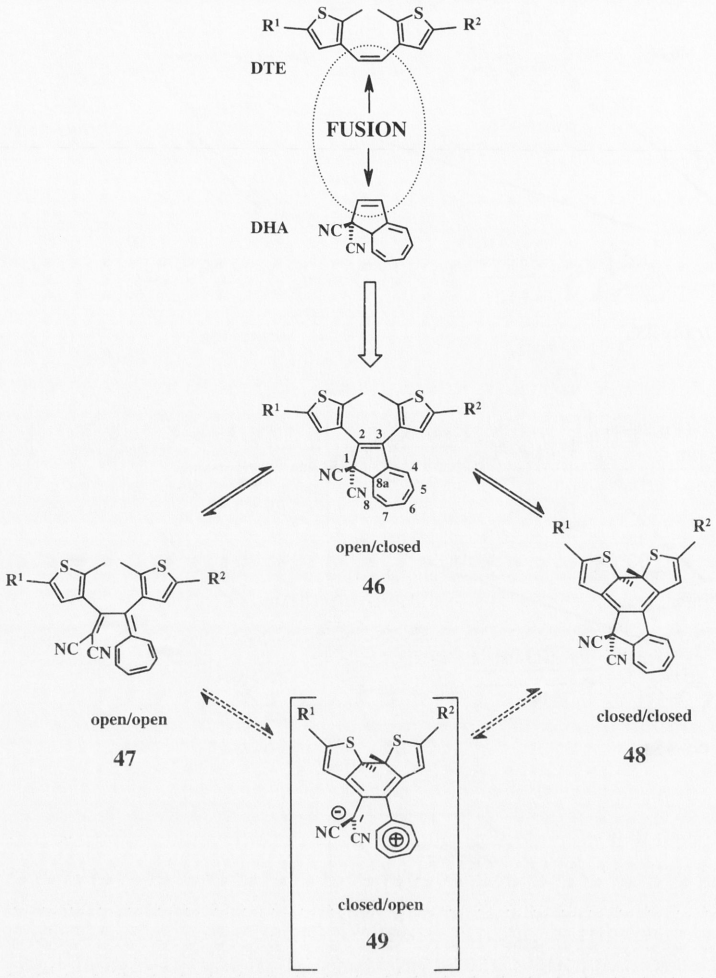

Scheme 11: Conception for a four-step cyclic process with biphotochromic compounds. The notation 'open/closed' for isomer **46** refers to the dithienyl moiety in its 'open' constitution and the dihydroazulene moiety in its 'closed' one. This notation applies equally to **47**, **48**, and **49**.

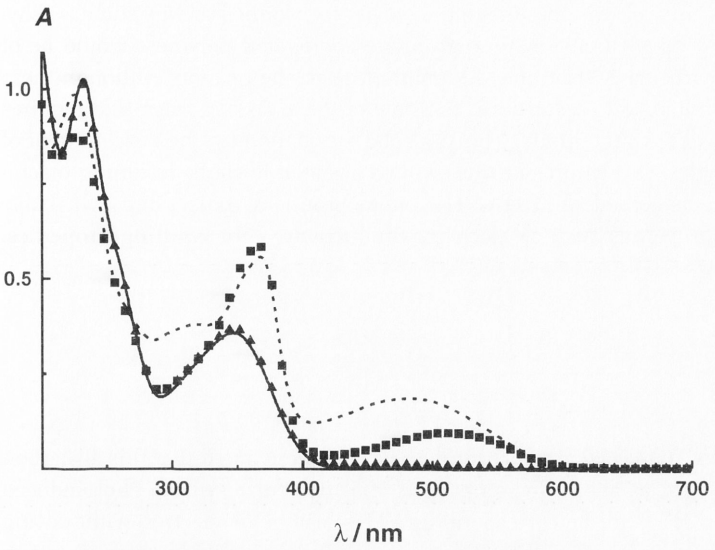

Fig. 35: Reversible irradiation of **46** in cyclohexane (4.4×10^{-5} mol dm^{-3}) at room temperature: **46** prior to (—) and after irradiation at 254 nm (- -), after thermal relaxation (■), and after subsequent irradiation with visible light (≥ 450 nm), in which **46** is restored (▲).

3.3
Future Directions

It has been predicted that what electrons did for the twentieth century, photons may do for the twenty-first. The reason is that photons can effect switching of properties in a shorter time scale and can carry information much more quickly, more efficiently, and over longer distances than electrons can. Therefore, considerable efforts have been directed in recent years toward the design of photoactive organic molecules, the physical properties of which can be manipulated by means of light. However, the major problems inherent in such molecules are their difficulties associated with device fabrication, due to a lack of processability and stability at various device operating conditions. On the other hand, polymers are more adaptable to structural manipulation and device fabrication and hence play a key role in the designing of advanced materials for optoelectronic and photonic devices. As a result, during the past decade, organic and polymer chemists have joined the quest to develop novel materials for various advanced technological applications. Even though there exist several studies pertaining to the use of photoswitchable organic molecules as photonic devices in combination with solid matrices such as polymers and sol-gels, their use as integral components of conjugated macromolecular systems to control the optoelectronic properties of the latter has not received adequate attention.[39] Processable and stable polymers possessing optoelectronic properties that can be controlled by photoswitches may well emerge as novel materials for optoelectronic

applications. In this context, the integration of photochromic systems such as dihydroazulenes and diarylethenes with appropriate conjugated polymers would be of great interest, particularly from the viewpoint of device fabrication. Although these areas imply technological applications, the state of the art is at a stage that requires considerable basic research input to build a solid foundation for the development of future technologies. Our future activities will be oriented towards designing macromolecular systems, based on **DHA-VHF** photochromism, possessing switchable optoelectronic properties such as electrical conductivity, light emitting properties, and NLO activity.

3.4 Conclusions

Recent studies of **DHA-VHF** photochromism have demonstrated that this all-carbon system can be used as an active component of a molecular switch. Photoinduced ring-opening of **DHA**s to the corresponding **VHF**s brings the electron-withdrawing cyano groups into conjugation with the π-system, thus engendering strong perturbations in electronic properties. Incorporation of appropriate functional moieties, possessing strong fluorescence and donor-acceptor interaction capabilities, into the **DHA-VHF** photochromic system can therefore lead to novel organic materials with switchable fluorescence, light emitting properties, and NLO activity. Nevertheless, the substitution and structure patterns currently in use do not allow for reversion of **VHF**s back into their corresponding **DHA**s on application of light of a different wavelength. Further molecular engineering studies to overcome this handicap will have to be performed in the future.

References

1 a) *Molecular Electronics: Some Directions* (Eds.: J. Jortner, M. Ratner), Blackwell, Oxford, UK, **1997**; b) *Molecular Electronics: Science and Technology* (Eds.: A. Aviram, M. Ratner), The New York Academy of Sciences, New York, **1998**.
c) *Molecular Electronics, Biosensors and Biocomputers* (Ed.: F. T. Houg), Plenum Press, New York, **1989**.

2 a) J.-M. Lehn, *Supramolecular Chemistry*, VCH, Weinheim, **1995**, pp. 124–138; b) M. P. Debreczeny, W. A. Svec, M. R. Wasielewski, *Science* **1996**, *274*, 584–587; c) V. Balzani, M. Gomez-Lopez, J. F. Stoddart, *Acc. Chem. Res.* **1998**, *31*, 305–414; d) W. A. Reinerth, L. Jones II, T. P. Burgin, C. Zhou, C. J. Muller, M. R. Deshpande, M. A. Reed, J. M. Tour, *Nanotechnology*, **1998**, *9*, 246–250; e) J.R. Sheats, P.F. Barbara, *Acc. Chem. Res.* **1999**, *32*, 191–192.

3 a) J. Daub, T. Knöchel, A. Mannschreck, *Angew. Chem.* **1984**, *96*, 980–981; *Angew. Chem., Int. Ed. Engl.* **1984**, *23*, 960–961; b) V. Balzani, F. Scandola in *Comprehensive Supramolecular Chemistry, Vol. 5* (Ed.: D. N. Reinhoudt), Pergamon-Elsevier, Oxford, **1996**, pp. 687–746; c) B. L. Feringa, W. F. Jager, B. de Lange, *Tetrahedron* **1993**, *49*, 8267–8310; d) *Photochromism, Molecules and Systems* (Eds.: H. Dürr, H. Bouas-Laurent), Elsevier, Amsterdam, **1990**; e) *Organic Photochromic and Thermochromic Compounds* (Eds.: J. C. Crano, R. J. Guglielmetti), Vol. *1* and Vol. *2*, Plenum Press, New York, **1999**; f) M. Grätzel, *Coord. Chem. Rev.* **1998**, *171*, 245–250.

4 a) A. P. de Silva, H. Q. N. Gunaratne, C. P. McCoy, *J. Am. Chem. Soc.* **1997**, *119*, 7891–7892; b) A. P. de Silva, H. Q. N. Gunaratne, T. Gunnlaugsson, A. J. M. Huxley, C. P. McCoy, J. T. Rademacher, T. E. Rice, *Chem Rev.* **1997**, *97*, 1515–1566; c) K. Rurack, M. Kollmannsberger, U. Resch-Genger, J. Daub, *J. Am. Chem. Soc.* **2000**, *122*, 968–969.

5 a) R. Bergonzi, L. Fabbrizzi, M. Licchelli, C. Mangano, *Coord. Chem. Rev.* **1998**, *170*, 31–46; b) J. Otsuki, K. Harada, K. Araki, *Chem. Lett.* **1999**, 269–270.

6 V. Goulle, A. Harriman, J. -M. Lehn, *J. Chem. Soc., Chem. Commun.* **1993**, 1034–1036.

7 K. Schaumburg in *Nanostructures Based on Molecular Materials* (Ed.: W. Göpel, C. Ziegler), VCH, Weinheim, **1992**, 153–173.

8 R. Deans, A. Niemz, E. C. Breinlinger, V. M. Rotello, *J. Am. Chem. Soc.* **1997**, *119*, 10863–10864.

9 I. Willner, *Acc. Chem. Res.* **1997**, *30*, 347–356.

10 J. Daub, M. Beck, A. Knorr, H. Spreitzer, *Pure Appl. Chem.* **1996**, *68*, 1399–1404.

11 a) M. Kollmannsberger, T. Gareis, S. Heinl, J. Breu, J. Daub, *Angew. Chem.* **1997**, 109, 1391–1393; *Angew. Chem., Int. Ed. Engl.* **1997**, *36*, 1333–1335, b) T. Werner, Ch. Huber, S. Heinl, M. Kollmannsberger, J. Daub, O. S. Wolfbeis, *Fresenius J. Anal. Chem.* **1997**, *359*, 150–154; c) M. Kollmannsberger, K. Rurack, U. Resch-Genger, J. Daub, *J. Phys. Chem. A.* **1998**, *102*, 10211–10220.

12 Z. Sekkat, W. Knoll, *Proc. SPIE-Int. Soc. Opt. Eng.* **1997**, *2998*, 164–184.

13 a) J. Whittal in *Photochromism: Molecules and Systems*, (Ed.: H. Dürr, H. Bouas-Laurent), Elsevier, Amsterdam, **1990**, 467–492; b) Y. C. Liang, A. S. Dvornikov, P. M. Rentzepis, *Res. Chem. Intermed*, **1998**, *24*, 905–914; c) P. J. Darcy, H. G. Heller, P. J. Strydom, J. Whittall, J. *Chem. Soc., Perkin Trans. I* **1981**, 202–205.

14 a) M. Irie, K. Uchida, *Bull. Chem. Soc. Jpn.* **1998**, *71*, 985–996; b) A. T. Bens, D. Frewert, K. Kodatis, C. Kryschi, H.-D. Martin, H. P. Trommsdorff, *Eur. J. Org. Chem.* **1998**, 2333–2338; c) M. Irie in Lit. 3e), Vol. *1*, 207–222.

15 J. Walz, K. Ulrich, H. Port, H. C. Wolf, J. Wonner, F. Effenberger, *Chem. Phys. Lett.* **1993**, *213*, 321–324.

16 a) T. Inada, S. Uchida, Y. Yokoyama, *Chem. Lett.* **1997**, 321–322; b) Y. Yokoyama, S. Uchida, Y. Yokoyama, Y. Sugawara, Y. Kurita, *J. Am. Chem. Soc.* **1996**, *118*, 3100–3107.

17 a) C. Weber, F. Rustemeyer, H. Dürr, *Adv. Mater.* **1998**, *10*, 1348–1351.

18 a) F. Pina, A. Roque, M. J. Melo, M. Maestri, L. Belladelli, V. Balzani, *Chem. Eur. J.* **1998**, *4*, 1184–1191; b) F. Pina, M. Maestri, V. Balzani, *Chem. Commun.* **1999**, 107–114; c) G. K. Faber, *Nat. Struct. Biol.* **1998**, *5*, 415–417; d) J. Vanhanen, V. P. Leppanen, T. Jaaskelainen, S. Parkkinen, J. P. S. Parkkinen, *Opt. Commun* **1998**, *153*, 289–294.

19 a) J. Daub, S. Gierisch, U. Klement, T. Knöchel, G. Mass, U. Seitz, *Chem. Ber.* **1986**, *119*, 2631–2646; b) S. Gierisch, J. Daub, *Chem. Ber.* **1989**, *122*, 69–75; c) S. Gierisch, W. Bauer, T. Burgemeister, J. Daub, *Chem. Ber.* **1989**, *122*, 2341–2349; d) J. Daub, T. Mrozek, A. Ajayaghosh, *Mol. Cryst. Liq. Cryst.* **2000**, *344*, 41–50.

20 J. Daub, C. Fischer, J. Salbeck, K. Ulrich, *Adv. Mater.* **1990**, *2*, 366–369.

21 a) H. Görner, C. Fischer, S. Gierisch, J. Daub, *J. Phys. Chem.* **1993**, *97*, 4110–4117; b) H. Görner, C. Fischer, J. Daub, *J. Photochem. Photobiol. A: Chem.* **1995**, *85*, 217–224; c) H. Mrozek, *PhD Thesis*, University of Regensburg, **1993**; d) M. Komma, *Diplomathesis*, University of Regensburg, **1996**.

22 a) O. Köthe, *PhD Thesis*, University of Regensburg, **1999**.

23 H. Spreitzer, J. Daub, *Liebigs. Ann.* **1995**, 1637–1641.

24 a) T. Mrozek, *PhD Thesis*, University of Regensburg, **2000**; b) A. Knorr, *Diploma Thesis*, University of Regensburg, **1992**, c) For recent results using femtosecond-resolved transient absorption spectroscopy, see: J. Ern, M. Petermann, T. Mrozek, J. Daub, K. Kuldova, C. Kryschi, *Chem. Phys.* **2000**, *259*, 331–337.

25 a) J. Daub, C. Fischer, S. Gierisch, J. Sixt, *Mol. Cryst. Liq. Cryst.* **1992**, *217*, 177–185; b) C. Fischer, J. Daub, *Chem. Ber.* **1993**, *126*, 1631–1634.

26 a) J. Daub, J. Salbeck, T. Knöchel, C. Fischer, H. Kunkely, K. M. Rapp, *Angew. Chem.* **1989**, *101*, 1541–1542; *Angew. Chem., Int. Ed. Engl.* **1989**, *28*, 1494–1496; b) J. Daub, K. M. Rapp, J. Salbeck, U. Schöberl in *Carbohydrates as Organic Raw Materials* (Ed.: F. W. Lichtenthaler), VCH, Weinheim, **1991**, pp.323–350.

27 J. Daub, S. Gierisch, J. Salbeck, *Tetrahedron Lett.* **1990**, *31*, 3113–3116.

28 a) M. Sisido in *Photo-React. Mater. Ultrahigh Density Opt. Mem.* (Ed.: M. Irie), Elsevier, Amsterdam, **1994**; b) N. P. M. Huck, W. F. Jager, B. de Lange, B. L. Feringa, *Science* **1996**, *273*, 1686–1688; c) L. Eggers, V. Buss, *Angew. Chem.* **1997**, *107*, 885–887; *Angew. Chem., Int. Ed. Engl.* **1997**, *36*, 881–883; d) K. S. Burnham, G. B. Schuster, *J. Am. Chem. Soc.* **1998**, *120*, 12619–12625; e) Y. Yokoyama, S. Uchida, Y. Yokoyama, T. Sagisaka; Y. Uchida, T. Inada, *Enantiomer* **1998**, *3*, 123–132; f) A. Mannschreck, K. Lorenz and M. Schinabeck in Lit. 3b), Vol. *2*, 261–295.

29 a) H. Rau, *Chem. Rev.* **1983**, *83*, 535–547; b) Y. Inoue, *Chem. Rev.* **1992**, *92*, 741–770; c) M. Sakamoto, M. Takahashi, T. Arai, M. Shimizu, T. Mino, S. Watanabe, T. Fujita, K. Yamaguchi, *J. Chem. Soc., Chem. Commun.* **1998**, 2315–2316; d) N. Koumura, N. Harada, *Chem. Lett.* **1998**, 1151–1152.

30 a) P. A. Bross, *PhD Thesis*, University of Regensburg, **1992**; b) G. Beer, *PhD Thesis*, University of Regensburg, **2001**.

31 J. Achatz, C. Fischer, J. Salbeck, J. Daub, *J. Chem. Soc., Chem. Commun.* **1991**, 504–507.

32 H. Spreitzer, J. Daub, *Chem. Eur. J.* **1996**, *2*, 1150–1158.

33 a) A. P. de Silva, C. P. McCoy, *Chem. Ind.* **1994**, 992–996; b) L. F. Lindon, *Nature* (London) **1993**, *364*, 17–18; c) A. Aviram, *J. Am. Chem. Soc.* **1988**, *110*, 5687–5692.

34 a) J. Bindl, P. Seitz, U. Seitz, E. Salbeck, J. Salbeck, J. Daub, *Chem. Ber.* **1987**, *120*, 1747–1756; b) M. Baumgarten, K. Müllen, *Top. Curr. Chem.* **1994**, *169*, 1–103.

35 a) J. Daub, M. Feuerer, A. Mirlach, J. Salbeck, *Synthetic Metals*, **1991**, *41–43*, 1551-1555; b) A. Mirlach, M. Feuerer, J. Daub, *Adv. Mater.* **1993**, *5*, 450–453; c) W. Schuhmann, J. Huber, A. Mirlach, J. Daub, *Adv. Mater.* **1993**, *5*, 124–126; d) M. Porsch, G. Sigl-Seifert, J. Daub, *Adv. Mater.* **1997**, *9*, 635–639; e) F. X. Redl, O. Köthe, K. Röckl, W. Bauer, J. Daub, *Macromol. Chem. Phys.* **2000**, *201*, 2091–2100.

36 P. A. Bross, A. Mirlach, J. Salbeck, J. Daub, *Dechema-Monographien* **1990**, *121*, 375–382.

37 L. Gobbi, P. Seiler, F. Diederich, *Angew. Chem.* **1999**, *111*, 737–740; *Angew. Chem., Int. Ed. Engl.* **1999**, *38*, 674–677.

38 a) T. Mrozek, H. Görner, J. Daub, *Chem. Commun.* **1999**, 1487–1488; b) T. Mrozek, H. Görner, J. Daub, *Chem. Eur. J.* **2001**, *7*, no. 5, 1028–1040.

39 Y. Atassi, J. Chauvin, J. A. Delaire, J.- F. Delouis, I. Fanton-Maltey, K. Nakatani, *Pure Appl. Chem.* **1998**, *70*, 2157–2166.